

# Efficient parameter sampling for Markov jump processes

Boqian Zhang and Vinayak Rao

*Department of Statistics, Purdue University, USA*

E-mail: zhan1977@purdue.edu, varao@purdue.edu

**Abstract.** Markov jump processes (MJPs) are continuous-time stochastic processes widely used in a variety of applied disciplines. Inference for MJPs typically proceeds via Markov chain Monte Carlo, the state-of-the-art being a uniformization-based auxiliary variable Gibbs sampler. This was designed for situations where the MJP parameters are known, and Bayesian inference over unknown parameters is typically carried out by incorporating it into a larger Gibbs sampler. This strategy of sampling parameters given path, and path given parameters can result in poor Markov chain mixing. In this work, we propose a simple and elegant algorithm to address this problem. Our scheme brings Metropolis-Hastings approaches for discrete-time hidden Markov models to the continuous-time setting, resulting in a complete and clean recipe for parameter and path inference in MJPs. In our experiments, we demonstrate superior performance over Gibbs sampling, as well as another popular approach, particle MCMC. We also show our sampler inherits geometric mixing from an ‘ideal’ sampler that operates without computational constraints.

*Keywords:* Markov jump process, Markov chain Monte Carlo, Metropolis-Hasting, Bayesian inference, Uniformization, Geometric Ergodicity

## 1. Introduction

Markov jump processes (MJPs) are continuous-time stochastic processes widely used in fields like computational chemistry [9], molecular genetics [7], mathematical finance [6], queuing theory [3], artificial intelligence [27] and social-network analysis [21]. These references have used MJPs to model temporal evolution of the state of a chemical reaction or queuing network, segmentation of a strand of DNA, user activity on social media, among many others, resulting in realistic, mechanistic, and interpretable models. These same continuous-time dynamics however raise computational challenges when, given noisy measurements, one wants to make inferences over the latent MJP trajectory as well as any parameters. In contrast to discrete-time hidden Markov models, one cannot *a priori* bound the number of state transitions, and the transition times themselves are continuous-valued. The state-of-the-art inference method for MJPs is an auxiliary variable Gibbs sampler from [25], we will refer to this as the Rao-Teh algorithm. This algorithm was designed to sample paths when the MJP parameters are known. Parameter inference is typically carried out by incorporating it into a Gibbs sampler that also conditionally simulates parameters given the currently sampled trajectory.

In many situations, the MJP trajectory and parameters exhibit strong coupling, so that alternately samples path given parameters, and parameters given path can result in poor mixing. To address this issue, we propose a simple, elegant and efficient Metropolis-Hastings framework. In our experiments, we demonstrate superior performance over

Gibbs sampling, as well as other approaches like particle Markov chain Monte Carlo [1]. We also prove that under relatively mild conditions, our sampler inherits geometric ergodicity from an ‘ideal’ sampler that operates without any computational constraints.

## 2. Markov jump processes (MJPs)

A Markov jump process [4] is a right-continuous piecewise-constant stochastic process  $S(t)$  taking values in a usually finite state space  $\mathcal{S}$ . We assume  $N$ -states, with  $\mathcal{S} = \{1, \dots, N\}$ . Then, the MJP is parameterized by two quantities, an  $N$ -component probability vector  $\pi_0$  and a rate-matrix  $A$ . The former gives the distribution over states at the initial time (we assume this is 0), while the latter is an  $N \times N$ -matrix governing the dynamics of the system. An off-diagonal element  $A_{ij}$ , for  $i \neq j$  gives the rate of transitioning from state  $i$  to  $j$ . The rows of  $A$  sum to 0, so that  $A_{ii} = -\sum_{j \neq i} A_{ij}$ . We write  $A_i$  for the negative of the  $i$ th diagonal element  $A_{ii}$ , so that  $A_i = -A_{ii}$  gives the total rate at which the system leaves state  $i$  for any other state. To simulate an MJP over an interval  $[0, t_{\text{end}}]$ , one follows Gillespie’s algorithm [9]: first sample an initial state  $s_0$  from  $\pi_0$ , and defining  $t_0 = t_{\text{curr}} = 0$  and  $k = 0$ , repeat the following while  $t_{\text{curr}} < t_{\text{end}}$ :

- Sample a wait-time  $\Delta t_k$  from an exponential distribution with rate  $A_{s_k}$ . Set  $t_{k+1} = t_{\text{curr}} + \Delta t_k$ . The MJP remains in state  $s_k$  until time  $t_{k+1}$ .
- Jump to a new state  $s_{k+1} \neq s_k$  with probability equal to  $A_{s_k s_{k+1}} / A_{s_k}$ . Set  $k = k + 1$ .

The times  $T = (t_0, \dots, t_{|T|-1})$  and states  $S = (s_0, \dots, s_{|T|-1})$  define the MJP path  $S(t)$ .

### 2.1. Structured rate matrices

While the rate matrix  $A$  can have  $N(N-1)$  independent elements, in typical applications, especially with large state-spaces, it is determined by a much smaller set of parameters. We will write these as  $\theta$ , with  $A$  a deterministic function of these parameters:  $A \equiv A(\theta)$ . The parameters  $\theta$  are often more interpretable than the elements of  $A$  and correspond directly to physical, biological or environmental parameters of interest. For example:

**Immigration-death processes** Here,  $\theta = (\alpha, \beta)$  with  $\alpha$  the arrival-rate and  $\beta$  the death-rate. The state represents the size of a population or queue. New individuals enter with rate  $\alpha$ , so off-diagonal elements  $A_{i, i+1}$  equal  $\alpha$ . Each individual dies at a rate  $\beta$ , so that  $A_{i, i-1} = i\beta$ . All other transitions have rate 0.

**Birth-death processes** This variant of the earlier MJP moves from state  $i$  to  $i + 1$  with rate  $i\alpha$ , with growth-rate proportional to population size. Again,  $\theta = (\alpha, \beta)$ .

**Codon substitution models** These characterize transitions between codons at a DNA locus over evolutionary time. In the simplest case, all transitions have the same rate [14], Other models group transitions into, e.g., ‘synonymous’ and ‘nonsynonymous’ transitions, that continue to or do not encode the same amino acid. These have their own rates, and as there are 61 codons, this gives a  $61 \times 61$  matrix determined by 2 parameters. More refined models [10] introduce additional parameters.

### 3. Bayesian inference for MJPs

#### 3.1. Trajectory inference given MJP parameters

This was addressed in [25] and extended to a broader class of jump processes in [24] (also see [7, 12, 5]). Both involve MJP path representations with auxiliary *candidate* jump times that are later *thinned*. We focus on the simpler, more popular Rao-Teh algorithm [25], based on the idea of simulating an MJP through *uniformization* [13].

Uniformization involves a parameter  $\Omega \geq \max_i A_i$ ; [25] suggest  $\Omega = 2 \max_i A_i$ . Unlike the sequential wait-and-jump Gillespie algorithm, first simulate a set  $W$  of candidate transition-times over  $[0, t_{end}]$  from a rate- $\Omega$  Poisson process.  $W$  defines a random grid on  $[0, t_{end}]$ . Define  $B = (I + \frac{1}{\Omega}A)$ ; this is a stochastic matrix with positive elements, and rows adding up to 1. Assign state-values to the elements in  $\{0\} \cup W$  according to a discrete-time Markov chain with initial distribution  $\pi_0$ , and transition matrix  $B$ . Call these states  $V$ . Thus  $v_0 \sim \pi_0$ , while  $P(v_{k+1} = j | v_k = i) = B_{ij}$  for  $k \in \{0, \dots, |W| - 1\}$ .  $\Omega > \max_i A_i$  results in more candidate-times than actual MJP transitions; at the same time, unlike  $A$ , the matrix  $B$  can thin these through self-transitions. Write  $U$  for the elements  $W$  with self-transitions, and  $T$  for the rest. Define  $S = \{v_i \in V \text{ s.t. } v_i \neq v_{i-1}\}$  as the elements in  $V$  corresponding to  $T$ , then  $(S, T)$  sampled this way for any  $\Omega \geq \max_i A_i$  has the same distribution as Gillespie's algorithm [13, 25]. Introducing the thinned variables allowed [25] to develop a novel, simple and efficient MCMC sampler. At a high-level, each MCMC iteration samples a new grid  $W$  conditioned on the trajectory  $S(t)$ , and then a new trajectory conditioned on the  $W$ . [25] show that the resulting Markov chain targets the desired posterior distribution over trajectories, and is ergodic for any choice of  $\Omega$  strictly greater than all the  $A_i$ 's.

---

**Algorithm 1** The Rao-Teh [25] auxiliary variable Gibbs sampler for MJP trajectories

---

**Input:** MJP parameters  $\theta$ ,  $\pi_0$ , observations  $X$ , the previous path  $S(t) = (S, T)$ .  
A parameter  $\Omega > \max_i A_i$ , where  $A = A(\theta)$  is the MJP rate-matrix.  
**Output:** A new MJP trajectory  $S'(t) = (S', T')$ .

---

- 1: **Given the MJP path  $(S, T)$ , sample a new set of thinned candidate times  $U$ :**  
These are distributed as an inhomogeneous Poisson process with intensity  $\Omega - A_{S(t)}$ . Since the intensity is piecewise-constant, simulating this is straightforward.
  - 2: **Given the thinned and actual transition times  $W = T \cup U$  from the previous iteration (after discarding state information  $S$ ), sample a new path  $V$ :**  
Conditioned on the skeleton  $W$ , the set of candidate jump times is fixed, and trajectory inference reduces to inference for a discrete-time hidden Markov model (HMM) with initial distribution  $\pi_0$ , and transition matrix  $B$ . [25] use the forward-filtering backward-sampling (FFBS) algorithm, an efficient dynamic programming algorithm that makes a forward pass through the finite set of times  $W$ , sequentially updating the distribution over states at each time  $w \in W$ . Between any two consecutive elements of  $W$ , the system remain in a fixed state, with the likelihood for a state  $s$  equal to the likelihood under state  $s$  of all observations in that interval. The end of the forward pass gives a distribution over states at the end time that accounts for all observations. The algorithm then makes a backward pass through the times in  $W$ , sequentially sampling the state  $v_i$  at time  $w_i$  given state  $v_{i+1}$  at time  $w_{i+1}$  and the corresponding distribution over states at  $w_i$  calculated during the forward pass.
-

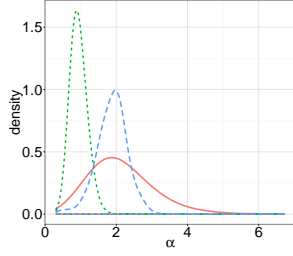


**Figure 1.** Prior distribution of an MJP parameter (the wide red density), as well as two conditional distributions. Narrow dotted-green is the density conditioned on both the observations as well as a simulated MJP posterior. The wider dashed-blue curve is density of interest: the marginal distribution of the parameters conditioned on observations. These plots were produced from the experiment in section 6.3.

### 3.2. Parameter inference for MJPs

For known parameters, the efficiency of the Rao-Teh algorithm has been established, both empirically [25] and theoretically [16]. In practice, the parameters are typically unknown: often, these are of primary interest when studying a dynamical system. A Bayesian approach places a prior  $p(\theta)$  over these, and the resulting posterior  $P(\theta|X)$  is typically approximated with samples drawn by Gibbs sampling. In particular, for an arbitrary initialization of path and parameters, one repeats the two steps from algorithm 2:

---

**Algorithm 2** Gibbs sampling for parameter inference for MJPs

---

**Input:** A set of partial and noisy observations  $X$ ,  
The previous MJP path  $S(t) = (S, T)$ , the previous MJP parameters  $\theta$ .  
**Output:** A new MJP trajectory  $S'(t) = (S', T')$ , new MJP parameters  $\theta'$ .

---

- 1: Sample a trajectory from the conditional  $P(S'(t)|X, S(t), \theta)$  by algorithm 1.
  - 2: Sample a new parameter  $\theta'$  from the conditional  $P(\theta'|X, S'(t))$ .
- 

The distribution  $P(\theta'|X, S(t))$  depends on a set of sufficient statistics of the MJP trajectory: how much time is spent in each state, and the number of transitions between each pair of states. In special circumstances,  $\theta$  can be directly sampled from its conditional distribution, otherwise, one has to use a Markov kernel like Metropolis-Hastings or Hamiltonian Monte Carlo to update  $\theta$  to  $\theta'$ . In any event, this introduces no new technical challenges. However, the Gibbs sampling approach comes with a well-known limitation: coupling between path and parameters can result in a very sluggish exploration of parameter and path space. We illustrate this in figure 1, which shows the posterior distribution of an MJP parameter (in dashed-blue) is less concentrated than the distribution conditioned on both observations as well the MJP trajectory (dotted-green). The coupling is strengthened as the trajectory grows longer, and the Gibbs sampler can mix very poorly for situations with long observation periods, even if the observations themselves are sparse and only mildly informative about the parameters.

For the discrete-time case, this problem of parameter-trajectory coupling can be circumvented by marginalizing out the MJP trajectory and directly sampling from the posterior over parameters  $P(\theta|X)$ . In its simplest form (Algorithm 3), this involves a Metropolis-Hastings scheme that proposes a new parameter  $\vartheta$  from some proposal distribution  $q(\vartheta|\theta)$ , accepting or rejecting according to the usual Metropolis-Hastings probability. The latter step requires calculating the marginal probabilities  $P(X|\theta)$  and  $P(X|\theta')$ , integrating out the exponential number of possible latent trajectories. Fortunately, this marginal probability is a by-product of the forward-backward algorithm used to sample a new trajectory, so that no additional computational burden is involved.

**Algorithm 3** Metropolis-Hastings parameter inference for a discrete-time Markov chain**Input:** Observations  $X$ , proposal density  $q(\vartheta|\theta)$ , and previous parameters  $\theta$ .**Output:** A new Markov chain parameter  $\theta'$ .

- 
- 1: Propose a new parameter  $\vartheta$  from the proposal distribution  $q(\vartheta|\theta)$ .
  - 2: Run the forward pass of the forward-backward algorithm to obtain the marginal likelihood of the observations,  $P(X|\vartheta)$ .
  - 3: Set  $\theta' = \vartheta$  with probability  $\min(1, \frac{P(X|\vartheta)q(\theta|\vartheta)}{P(X|\theta)q(\vartheta|\theta)})$ , else  $\theta' = \theta$ .
  - 4: Sample a new path with the backward pass of the forward-backward algorithm.
- 

**3.3. A marginal sampler for MJP parameters**

Constructing a marginal sampler over the MJP parameters by integrating out the continuous-time trajectory is harder. One approach [7] makes a sequential forward pass through all *observations*  $X$ , using matrix exponentiation to marginalize out all continuous-time paths between successive times. As shown in [25], this approach is cubic rather than quadratic in the number of states, cannot exploit structure like sparsity in the transition matrix, and can depend in not trivial ways on the exact nature of the observation process. Also, the number of expensive matrix exponentiations depends on the number of observations rather than the number of transitions. A second approach, particle MCMC [1], uses particle filtering to get an unbiased estimate of the marginal  $P(X|\theta)$ . Plugging this into the Metropolis-Hastings acceptance probability results in an MCMC sampler that targets the correct posterior, however the resulting scheme does not exploit the structure of the MJP, and we show that it is quite inefficient.

[25, 24] demonstrated the advantage of introducing the thinned events  $U$ : this allows exploiting discrete-time algorithms like FFBS for path sampling. In the next section, we outline a naïve first attempt at extending this approach to parameter inference. We describe why this approach is not adequate, and then describe our final algorithm.

**4. Naïve parameter inference via Metropolis-Hastings**

The Rao-Teh algorithm [25] simplifies computation by conditioning on the random grid  $W$ . This suggests conditioning on  $W$  to update the parameters as well, following the scheme from Algorithm 3. In particular, given  $W$ , discard all state information, and propose a new parameter  $\vartheta$  from  $q(\vartheta|\theta)$ . The MH-acceptance probability is  $\min\left(1, \frac{P(X|W, \vartheta)P(W|\vartheta)p(\vartheta)q(\theta|\vartheta)}{P(X|W, \theta)P(W|\theta)p(\theta)q(\vartheta|\theta)}\right)$ ; to calculate it, make a forward pass over  $W$ , and calculate  $P(X|W, \theta)$  and  $P(X|W, \vartheta)$ . After accepting or rejecting  $\vartheta$ , the new parameter  $\theta'$  is used in a backward pass that samples a new trajectory. Then discard all self-transitions, resample  $W$  and repeat. Algorithm 4, and figure 11 in the appendix sketch this out.

The resulting algorithm updates  $\theta$  with the MJP trajectory integrated out, giving more rapid mixing. However  $\theta$  is still updated *conditioned on*  $W$ , and the distribution of  $W$  depends on  $\theta$ :  $W$  is a homogeneous Poisson process with rate  $\Omega(\theta)$ . The fact that the MH-acceptance probability involves a  $P(X|\theta)$  term is inevitable, however we found that the  $P(W|\theta)$  terms significantly affects acceptance probabilities. Any proposal that halves  $\Omega(\theta)$  will halve the mean and variance of the distribution of the number of events in  $W$ , resulting in a low acceptance probability. This will affect mixing. The next section describes an algorithm to get around this.

**Algorithm 4** Naïve MH for parameter inference for MJPs

**Input:** Observations  $X$ , the MJP path  $S(t) = (S, T)$ , the parameters  $\theta$  and  $\pi_0$ .  
A Metropolis-Hasting proposal  $q(\cdot|\theta)$ .

**Output:** A new MJP trajectory  $S'(t) = (S', T')$ , new MJP parameters  $\theta'$ .

- 1: Set  $\Omega \doteq \Omega(\theta) > \max_s A_s(\theta)$  for some function  $\Omega(\cdot)$  (e.g.  $\Omega(\theta) = 2 \max_s A_s(\theta)$ ).
- 2: Sample thinned jumps  $U \subset [0, t_{end}]$  from a Poisson process with piecewise-constant rate  $R(t) = (\Omega - A_{S(t)})$ . Set  $W = T \cup U$  and discard MJP state information.
- 3: Propose  $\vartheta \sim q(\cdot|\theta)$ . The acceptance probability is given by

$$\alpha = 1 \wedge \frac{P(\vartheta|W, X) q(\theta|\vartheta)}{P(\theta|W, X) q(\vartheta|\theta)} = 1 \wedge \frac{P(X|W, \vartheta)P(W|\vartheta)p(\vartheta) q(\theta|\vartheta)}{P(X|W, \theta)P(W|\theta)p(\theta) q(\vartheta|\theta)}.$$

- 4: For both  $\theta$  and  $\vartheta$ , make a forward pass through the elements of  $W$ , sequentially updating the distribution over states at  $w \in W$  given observations up to  $w$ . For any  $\theta$ , the transition matrix  $B(\theta)$  equals  $I + \frac{A(\theta)}{\Omega(\theta)}$  while the initial distribution over states is  $\pi_0$ . The likelihood of state  $s$  at step  $i$  is  $L_i(s) = P(X_{[w_i, w_{i+1})}|S(t) = s, t \in [w_i, w_{i+1}))$ , where  $X_{[w_i, w_{i+1})}$  is all observation lying in  $[w_i, w_{i+1})$ . At the end, we have  $P(X|W, \theta)$  and  $P(X|W, \vartheta)$ . Use these, and the fact that  $P(W|\theta)$  is Poisson-distributed to accept or reject the proposed  $\vartheta$ . Write the new parameter as  $\theta'$ .
- 5: For the new parameter  $\theta'$ , make a backward pass through the elements of  $W$ , sequentially assigning a state to each element of  $W$ . This completes the FFBS algorithm.
- 6: Let  $T'$  be the set of times in  $W$  when the Markov chain changes state. Define  $S'$  as the corresponding set of state values. Return  $(S', T', \theta')$ .

**5. An improved Metropolis-Hasting algorithm**

Our main idea is to symmetrize the probability of  $W$  under the old and proposed parameters, so that  $P(W|\theta)$  disappears from the acceptance ratio. This results in a significantly more efficient, and also a simpler MCMC scheme. As before, the MCMC iteration begins with the pair  $(S(t), \theta)$ . Instead of simulating the Poisson events  $U$ , we first generate a new parameter  $\vartheta$  from  $q(\vartheta|\theta)$ . Treat this as an auxiliary variable, so that the augmented space now is the triplet  $(S(t), \theta, \vartheta)$ . We pretend  $S(t) \equiv (S, T)$  was sampled by uniformization, where the dominating Poisson rate  $\Omega$  equals  $(\Omega(\theta) + \Omega(\vartheta))$  instead of just  $\Omega(\theta)$  (recall any choice greater than  $\max_s A_s$  is valid). Now the set of thinned events  $U$  is piecewise-constant Poisson with intensity  $\Omega(\theta) + \Omega(\vartheta) - A_{S(t)}$ . Following algorithm 1 or [25], the *a priori* probability of the reconstructed set  $W = U \cup T$ ,  $P(W|\theta, \vartheta)$ , is a homogeneous Poisson process with rate  $\Omega(\theta) + \Omega(\vartheta)$ . Discard all MJP state information, so that the MCMC state space is  $(W, \theta, \vartheta)$ , and propose swapping  $\theta$  with  $\vartheta$ . Observe from symmetry that the Poisson skeleton  $W$  has the same probability both before and after this proposal, so that unlike the previous scheme, the ratio  $P(W|\vartheta)/P(W|\theta)$  equals 1. This simplifies computation, and significantly improves mixing. The acceptance probability equals  $\min\left(1, \frac{P(X, \vartheta)q(\theta|\vartheta)}{P(X, \theta)q(\vartheta|\theta)}\right) = \min\left(1, \frac{P(X|\vartheta)p(\vartheta)q(\theta|\vartheta)}{P(X|\theta)p(\theta)q(\vartheta|\theta)}\right)$ . The terms  $P(X|\vartheta)$  and  $P(X|\theta)$  can be calculated by running a forward pass of the forward-backward algorithm, and after accepting or rejecting the proposal, a new trajectory is sampled by completing the backward pass. Finally, the thinned events are discarded. We sketch out our algorithm in Algorithm 5 and figure 12 in the appendix.

**Algorithm 5** Symmetrized MH for parameter inference for MJPs

**Input:** The observations  $X$ , the MJP path  $S(t) = (S, T)$ , parameters  $\theta$  and  $\pi_0$ .  
A Metropolis-Hasting proposal  $q(\cdot|\theta)$ .

**Output:** A new MJP trajectory  $S'(t) = (S', T')$ , new MJP parameters  $\theta'$ .

- 1: Sample  $\vartheta \sim q(\cdot|\theta)$ , and set  $\Omega \doteq \Omega(\theta) + \Omega(\vartheta)$  for some function  $\Omega(\theta) \geq \max_s A_s(\theta)$ .
- 2: Sample thinned jumps  $U \subset [0, t_{end}]$  from a Poisson process with piecewise-constant rate  $R(t) = (\Omega - A_{S(t)}(\theta))$ . Set  $W = T \cup U$  and discard MJP states.
- 3: The current MCMC state-space is  $(W, \theta, \vartheta)$ . Propose swapping  $\theta$  and  $\vartheta$ . The acceptance probability is given by

$$\alpha = 1 \wedge \frac{P(X|W, \vartheta, \theta)p(\vartheta)q(\theta|\vartheta)}{P(X|W, \theta, \vartheta)p(\theta)q(\vartheta|\theta)}.$$

- 4: For both  $\theta$  and  $\vartheta$ , make a forward pass through the elements of  $W$ , sequentially updating the distribution over states at  $w \in W$  given observations up to  $w$ . At the end, we have calculated  $P(X|W, \theta, \vartheta)$  and  $P(X|W, \vartheta, \theta)$ . Use these to accept or reject the proposed swapping of  $\theta$  and  $\vartheta$ . Write the new state-space as  $(W, \theta', \vartheta')$ .
- 5: For the new transition matrix  $B(\theta', \vartheta')$ , make a backward pass through the elements of  $W$ , sequentially assigning a state to each element  $w_i \in W$  given  $w_{i+1}$ .
- 6: Let  $T'$  be the set of times in  $W$  when the Markov chain changes state. Define  $S'$  as the corresponding set of state values. Return  $(S', T', \theta')$ .

PROPOSITION 1. *The sampler described in Algorithm 5 has the posterior distribution  $P(\theta, S(t)|X)$  as its stationary distribution.*

PROOF. Suppose that at the start of the algorithm, we have a pair  $(\theta, S(t))$  from the posterior distribution  $P(\theta, S(t)|X)$ . Introducing  $\vartheta$  from  $q(\vartheta|\theta)$  results in a triplet whose marginal over the first two variables is still  $P(\theta, S(t)|X)$ .

Sampling  $U$  from a Poisson process with rate  $\Omega(\theta) + \Omega(\vartheta) - A_{S(t)}(\theta)$ , results in a random grid  $W = T \cup U$  that is distributed according to a rate  $\Omega(\theta) + \Omega(\vartheta)$  Poisson process (Proposition 2 in [25]). Discarding all state information results in a triplet  $(W, \theta, \vartheta)$  with probability proportional to  $p(\theta)q(\vartheta|\theta)P(W|\theta, \vartheta)P(X|W, \theta, \vartheta)$ .

Next we propose swapping  $\theta$  and  $\vartheta$ . Since this is a deterministic proposal, the MH-acceptance probability is given by

$$\alpha = 1 \wedge \frac{p(\vartheta)q(\theta|\vartheta)P(W|\vartheta, \theta)P(X|W, \vartheta, \theta)}{p(\theta)q(\vartheta|\theta)P(W|\theta, \vartheta)P(X|W, \theta, \vartheta)}$$

The term  $P(W|\theta, \vartheta)$  is just a Poisson process with rate  $\Omega(\theta) + \Omega(\vartheta)$ , so that  $P(W|\theta, \vartheta) = P(W|\theta, \vartheta)$ .  $P(X|W, \theta, \vartheta)$  and  $P(X|W, \vartheta, \theta)$  are obtained after a forward pass over  $W$  using discrete-time transition matrices  $B(\theta, \vartheta) = \left(I + \frac{A(\theta)}{\Omega(\theta) + \Omega(\vartheta)}\right)$  and  $B(\vartheta, \theta) = \left(I + \frac{A(\vartheta)}{\Omega(\theta) + \Omega(\vartheta)}\right)$ .

Calling the parameters after the accept step  $(\theta', \vartheta')$ , we have that  $(\theta', \vartheta', W)$  has the same distribution as  $(\theta, \vartheta, W)$ . Finally, following Lemma 1 in [25], using the matrix  $B(\theta, \vartheta)$  to make a backward pass through  $W$ , and discarding the self-transitions results in a trajectory  $(S'(t))$  distributed according to  $A(\theta')$ . Discarding the auxiliary parameter  $\vartheta'$  results in a pair  $(\theta', S'(t))$  from the posterior distribution.  $\square$

### 5.1. Comments

The uniformization scheme of [25] works for any underlying Poisson process whose rate  $\Omega$  is greater than  $\max_i A_i$ . The strict inequality ensures that the conditional probability of sampling one or more thinned events  $U$  is positive for every trajectory  $S(t)$  (recall  $U \sim \text{PoissonProc}(\Omega - A_{S(t)})$ ). Empirical results from [25] suggest setting  $\Omega = 2 \max_i A_i$ .

Implicit in our new scheme is a uniformizing Poisson process with rate  $\Omega(\theta, \vartheta) = \Omega(\theta) + \Omega(\vartheta)$ . For our scheme to be valid,  $\Omega(\theta, \vartheta)$  must be greater than both  $\max_i A_i(\theta)$  and  $\max_i A_i(\vartheta)$ . The smallest and simplest such choice is  $\Omega(\theta, \vartheta) = \max A_i(\theta) + \max A_i(\vartheta)$ . For a fixed  $\theta$ , this reduces to  $\Omega = 2 \max A_i$ , providing an principled motivation for the approach in [25]. Larger alternatives include  $\Omega(\theta, \vartheta) = \kappa(\max A_i(\theta) + \max A_i(\vartheta))$  for  $\kappa > 1$ . These result in more thinned events, and so more computation, with the benefit of faster MCMC mixing. We study the effect of  $\kappa$  in our experiments. It is also possible to have non-additive settings for  $\Omega(\theta, \vartheta)$ , for example, setting  $\Omega(\theta, \vartheta)$  to  $\kappa \max(\max_i A_i(\theta), \max A_i(\vartheta))$  for some choice of  $\kappa > 1$ . We investigate this as well.

Our proposed algorithm is related to work on MCMC inference for doubly-intractable distributions. Algorithms like [17, 18, 2] all attempt to evaluate an intractable likelihood under a proposed parameter  $\vartheta$  by introducing auxiliary variables, however there the auxiliary variable is sampled independently under the proposed parameters. For MJP, this would involve proposing a new parameter  $\vartheta$ , generating a new uniformizing grid  $U^*$ , and then accepting or rejecting. This can complicate computations (with two sets of time points), and also reduce acceptance rates if the new parameter  $\vartheta$  is incompatible with the old grid  $U$  or vice versa. While [18] suggest annealing schemes to try to address this issue, we exploit the structure of the Poisson process and provide a cleaner solution: generate a single set of auxiliary variables that depends symmetrically on both the new and old parameters. It is interesting to see whether a similar idea can be used in other applications as well.

## 6. Experiments

In the following, we evaluate Python implementations of our two proposed algorithms, the naïve MH algorithm (Algorithm 4, which we plot in yellow) and its symmetrized improvement (Algorithm 5, which we call symmetrized MH and plot in red). We compare different variants of these algorithms, corresponding to different uniformizing Poisson rates (i.e. different choices of  $\kappa$ , see section 5.1). For naïve MH, we set  $\Omega(\theta) = \kappa \max_s A_s(\theta)$  with  $\kappa$  equal to 1.5, 2 and 3, represented in our plots with circles, triangles and square symbols. For symmetrized MH, where the uniformizing rate depends on both the current and proposed parameter, we consider two settings  $\Omega(\theta, \vartheta) = \kappa(\max A(\theta) + \max A(\vartheta))$  ( $\kappa = 1$  and 1.5, plotted with triangles and squares), and  $\Omega(\theta, \vartheta) = \kappa \max(\max A(\theta), \max A(\vartheta))$  ( $\kappa = 1.5$ , plotted with circles). We compare these algorithms against two baselines: Gibbs sampling (Algorithm 2, plotted in blue), and particle MCMC [1], plotted in black. Gibbs sampling involves a uniformization step to update the MJP trajectory, and for this we used three settings,  $\kappa = 1.5, 2, 3$ , plotted with circles, triangles and squares. Unless specified, our results were obtained from 100 independent MCMC runs, each consisting of 10000 iterations. We found particle MCMC to be more computationally intensive, and limited each run to 3000 iterations, the number of particles being 5, 10 and 20 (plotted with circles, triangles and squares).



For each run of each MCMC algorithm, we calculated the effective sample size (ESS) of the posterior samples of the MJP parameters using the R package `rcoda` [23]. This estimates the number of independent samples returned by the MCMC algorithm, and dividing this by the runtime of a simulation gives the ESS per unit time. We used this measure to compare different samplers and different parameter settings.

### 6.1. A simple synthetic MJP

Consider an MJP with two parameters  $\alpha$  and  $\beta$ , transitions between states  $i$  and  $j$  having rate  $\alpha \exp(-\beta/(i+j))$ . We consider three settings: 3 states (figure 2), 5 states, and 10 states. We place  $\text{Gamma}(\alpha_0, \alpha_1)$ , and  $\text{Gamma}(\beta_0, \beta_1)$  priors on the parameters  $\alpha$  and  $\beta$ , with  $(\alpha_0, \alpha_1, \beta_0, \beta_1)$  having values  $(3, 2, 5, 2)$  respectively. For each run, we draw random parameters from the prior to construct a transition matrix  $A$ , and placing a uniform distribution over states at time 0, simulate an MJP trajectory. We simulate observations uniformly at integer values on the time interval  $[0, 20]$ . Each observation is Gaussian distributed with mean equal to the state at that time, and variance equal to 1. For the Metropolis-Hastings proposal, we used a lognormal distribution centered at the current parameter value, with variance  $\sigma^2$  that we vary.

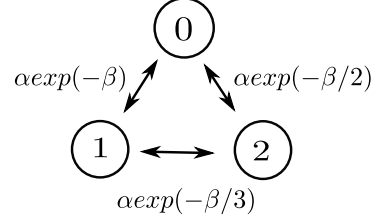


**Figure 2.** A 3-state MJP with exponentially decaying rates

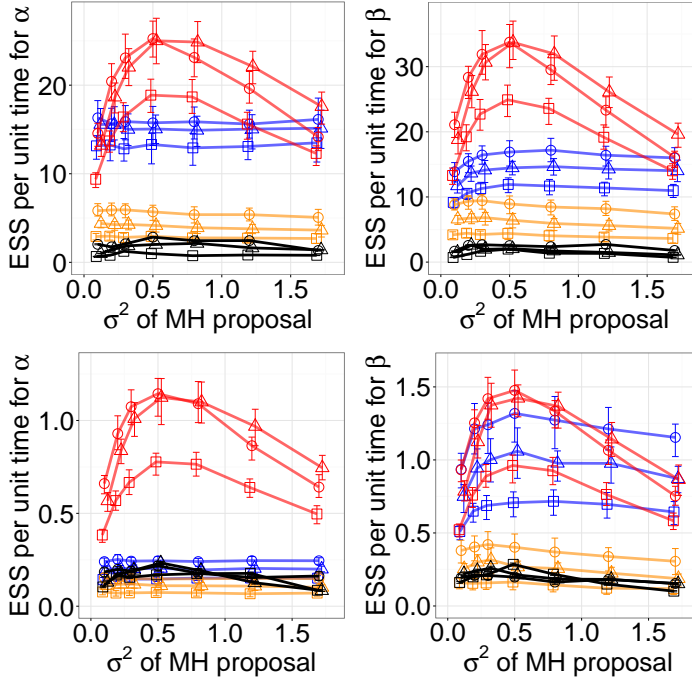


**Figure 3.** ESS/sec for the synthetic model, the top row being dimension 3, and the bottom, dimension 10. The left column is for  $\alpha$ , and the right is for  $\beta$ . Red, yellow, blue and black curves are the symmetrized MH, naïve MH, Gibbs and particle MCMC algorithm. Different symbols correspond to different settings of the algorithms, see section 6

**Results:** Figure 3 plots the ESS per unit time for the parameters  $\alpha$  (left) and  $\beta$  (right) for the case of 3 states (top row) and 10 states (bottom row) as we vary the scale-parameter  $\sigma^2$  of the log-normal proposal distribution. We include results for 5 states in

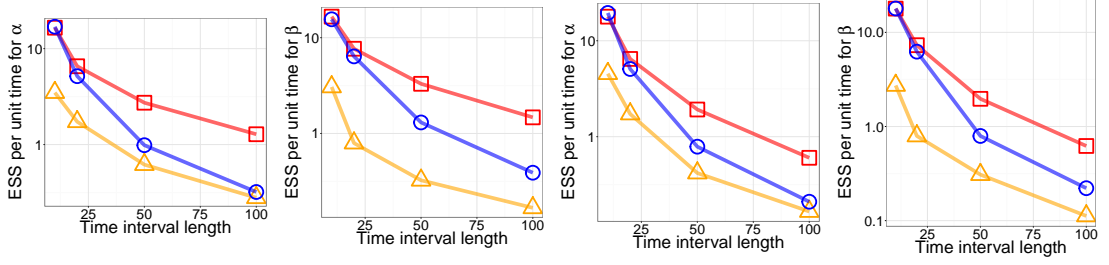


**Figure 4.** Time Interval vs. ESS/sec. In the left two plots, the number of observations is fixed, in the right two, this grows linearly with the interval length. Red (square), yellow (triangle) and blue (circle) curves are the symmetrized MH, naïve MH and Gibbs algorithm.

the appendix, the conclusions are the same. We see that our symmetrized MH algorithm is significantly more efficient than the baselines over a wide range of choices of  $\sigma^2$ , (including the natural choice of 1). Among the three setting of our algorithm, the simple additive setting (triangles) does best, though it is only slightly better than the max-of-max setting (circles). A reason for this improvement is that the additive setting is more stable than the max-of-max setting, when the proposal variance can be large. The additive setting with a multiplicative factor of 1.5 (squares) does worse than both additive choice with smaller multiplicative factor and the max-of-max choice but still better than the other algorithms. Among the baselines, simple Gibbs sampling does better than naïve Metropolis-Hastings, suggesting that the dependency of the Poisson grid on the MJP parameters does indeed significantly slow down mixing. Particle MCMC has the worst performance for this task. The results in figure 3 for the 10-dimensional state space show that for the parameter  $\alpha$ , the improvement that our proposed sampler affords is even more dramatic. For the parameter  $\beta$  however, performance is comparable to Gibbs, although it is not possible to claim one is uniformly superior to the other.

In figure 4, we plot ESS per unit time as the observation interval  $t_{end}$  increases. We consider the three-state MJP, and as before there are 19 observations uniformly located over a time interval  $(0, t_{end})$ . We consider four settings, with  $t_{end}$  equal to 10, 20, 50, 100. For each, we compare our symmetrized MH sampler (with  $\kappa$  set to 1) with the Gibbs sampler (with  $\kappa$  set to 2). While the performance of the Gibbs sampler is comparable with our symmetrized algorithm for the smallest value of  $t_{end}$ , its performance is considerably worse for longer time-intervals. This is because the Gibbs sampler updates  $\theta$  conditioned on the MJP trajectory, and longer time intervals result in stronger coupling between MJP path and parameters, and thus poorer mixing. This effect disappears if we integrate out the MJP trajectory. This experiment demonstrates that it is not sufficient just to integrate out the state values of the trajectory, we also have to get around the effect of the trajectory transition times. Our symmetrized MH-algorithm allows this.

To the right of figure 4, we plot results from a similar experiment. Now, instead of keeping the number of measurements fixed as we increase the observation interval, we keep the observation rate fixed at one observation every unit interval of time, so that longer observation intervals have larger number of observations. The results are similar to the previous case: Gibbs sampling performs well for small observation intervals, with

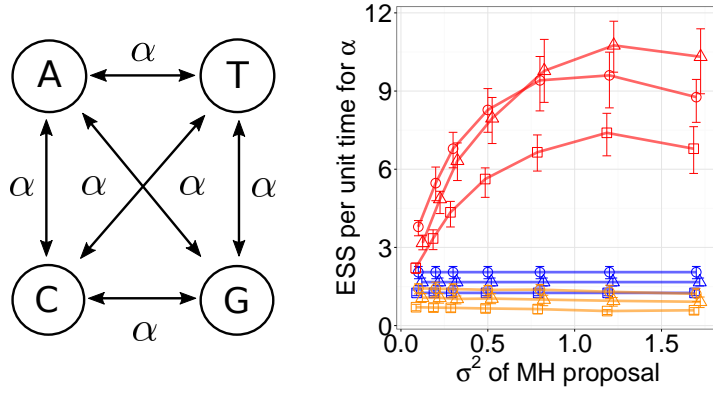


**Figure 5.** (a) Jukes-Cantor (JC69) model, (b) ESS/sec for the JC69 Model. Red, yellow and blue curves are the symmetrized MH, naïve MH and Gibbs algorithm.

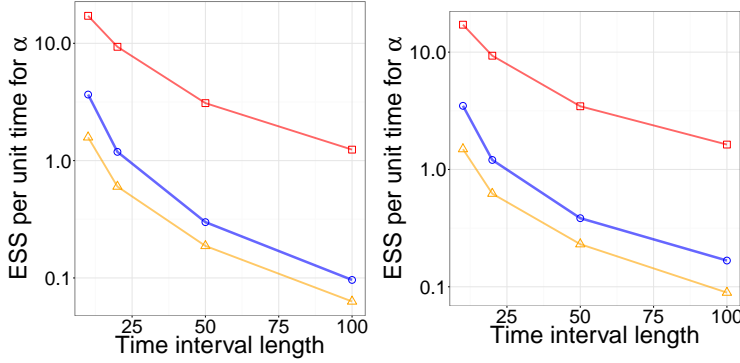


**Figure 6.** Time Interval vs. ESS/sec for JC model. In the left plot, the number of observations is fixed, in the right, this grows linearly with the interval length. Red, yellow and blue curves are the symmetrized MH, naïve MH and Gibbs.

performance degrading sharply for larger intervals. These two experiments illustrate the importance of integrating out the MJP path while carrying out parameter inference.

## 6.2. The Jukes and Cantor (JC69) model

The Jukes and Cantor (JC69) model [14] is a popular model of DNA nucleotide substitution. We write its state space as  $\{0, 1, 2, 3\}$ , representing the four nucleotides  $\{A, T, C, G\}$ . The model has a single parameter  $\alpha$ , representing the rate at which the system transitions between any pair of states. Thus, the rate matrix  $A$  is given by  $A_{ii} = -A_{i,i} = 3\alpha$ ,  $A_{i,j} = \alpha$ ,  $i \neq j$ . We place a  $\text{Gamma}(3, 2)$  prior on the parameter  $\alpha$ . Figure 5(right) compares different samplers: we see that the symmetrized MH samplers comprehensively outperforms all others. Part of the reason why the difference is so dramatic here is because the transition matrix is no longer sparse in this example, implying a stronger coupling between MJP path and parameter  $\alpha$ . We point out that for Gibbs sampling, the conditional parameter update is conjugate, and there is no proposal distribution involved (hence its performance remains fixed along the x-axis). Particle MCMC performs worse than all the algorithms, and we do not include it in our plots.

In figure 6, we plot the ESS per unit time for the different samplers as we increase the observation interval. In the left plot, we keep the number of observations fixed, in the right, these increase with the observation interval. Once again we see that our proposed algorithm 1) performs best over all interval lengths, and 2) suffers a performance degradation with interval length that is much milder than the other algorithms.

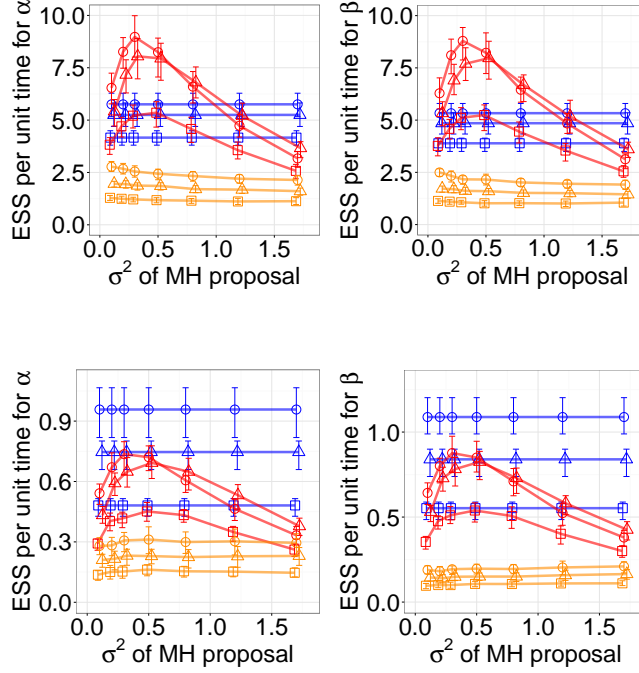


**Figure 7.** ESS/sec for the immigration model, the top row being dimension 3, and the bottom, dimension 10. The left column is for  $\alpha$ , and the right is for  $\beta$ . Red, yellow, and blue curves are the symmetrized MH, naïve MH, Gibbs sampling and particle MCMC.

### 6.3. An immigration model with finite capacity

Next, we consider an M/M/N/N queue [11]. The state space of this is stochastic process is  $\{0, 1, 2, 3, \dots, N-1\}$  with elements giving the number of customers/jobs/individuals in a system/population. Arrivals follow a rate- $\alpha$  Poisson process, moving the process from state  $i$  to  $i+1$  for  $i < N$ . The system has a capacity of  $N$ , so any arrivals when the current state is  $N$  are discarded. Service times or deaths are exponentially distributed, with a rate that is now state-dependent: the system moves from  $i$  to  $i-1$  with rate  $i\beta$ .

We follow the same setup as the first experiment: for  $(\alpha_0, \alpha_1, \beta_0, \beta_1)$  equal to  $(3, 2, 5, 2)$ , we place  $\text{Gamma}(\alpha_0, \alpha_1)$ , and  $\text{Gamma}(\beta_0, \beta_1)$  priors on  $\alpha, \beta$ . These prior distributions are used to sample transition matrices  $A$ , which, along with a uniform distribution over initial states, are used to generate MJP trajectories. We observe these at integer-valued times according to a Gaussian observation process. We consider three settings: 3, 5 and 10 states, with results from 5 steps included in the appendix.

Figure 7 plots the ESS per unit time for the parameters  $\alpha$  (left) and  $\beta$  (right) as we change the variance of the proposal kernel, for different settings of different algorithms. The top row shows results for a state-space of dimension 3, and the bottom row, results for a dimension 10. Again, our symmetrized MH algorithm does best for dimensions 3 and 5, although now Gibbs sampling performs well for dimensionality 10. This is partly because for this problem, the Gibbs conditionals over  $\alpha$  and  $\beta$  are conjugate, and have a very simple Gamma distribution (this is also why the Gibbs sampler curves are straight lines: there is no proposal distribution involved here).

**A time-inhomogeneous immigration model:** We extend the previous model to incorporate a known time-inhomogeneity. The arrival and death rates are no longer constant, and are instead given by  $A_{i,i+1}(t) = \alpha w(t)$  ( $i = 0, 1, \dots, N-1$ ) respectively.

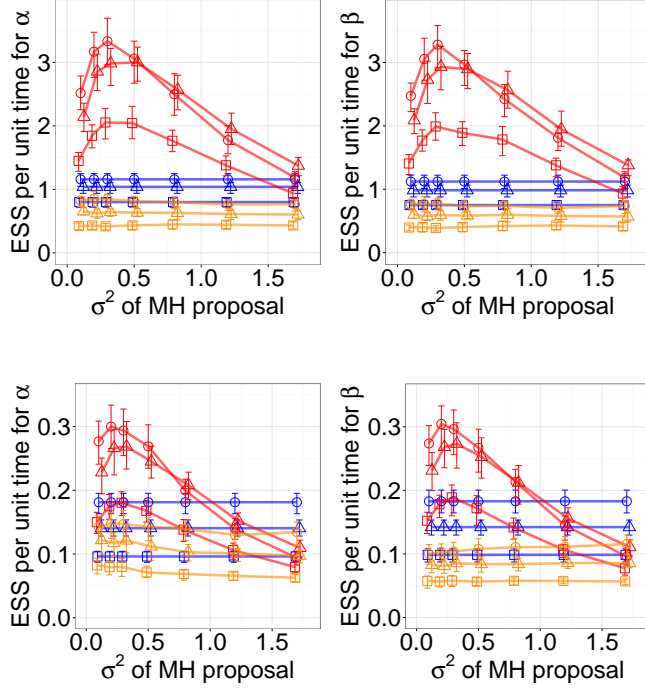


**Figure 8.** ESS/sec for the time-inhomogeneous immigration model, the top row being dimension 3, and the bottom, dimension 10. The left column is for  $\alpha$ , and the right is for  $\beta$ . Red, yellow and blue curves are the symmetrized MH, naïve MH, and Gibbs algorithm.

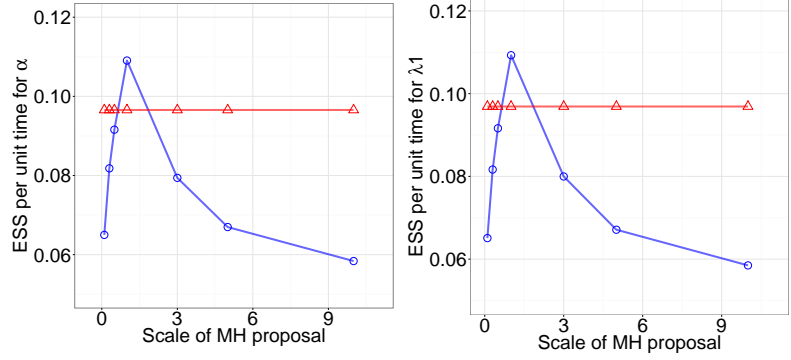
While it is not difficult to work with sophisticated choices of  $w(t)$ , we limit ourselves to a simple piecewise-constant  $w(t) = \lfloor \frac{t}{5} \rfloor$ . Even such a simple change in the original model can dramatically affect the performance of the Gibbs sampler.

The top row of figure 8 plots the ESS per unit time for the parameters  $\alpha$  (left) and  $\beta$  (right) for the immigration model with capacity 3. Now, the symmetrized MH algorithm is significantly more efficient, comfortably outperforming all samplers (including the Gibbs sampler) over a wide range of settings. Figure 8 shows performance for dimension 10, once again the symmetrized MH-algorithm performs best over a range of settings of the proposal variance. We note that increasing the dimensionality of the state space results in a more concentrated posterior, shifting the optimal setting of the proposal variance to smaller values.

#### 6.4. Chi-site data for *Escherichia coli*

We consider a dataset of *E. coli* DNA used in [7]. This consists of positions of Chi sites (motifs of eight base pairs, GCTGGTGG) along the inner (lagging) strand of the *E. coli* genome. Following [7], we wish to use this data to infer a two-state piecewise-constant segmentation of the DNA strand. We place a MJP prior over this segmentation, and indexing position along the strand with  $t$ , we write this as  $S(t)$  ( $t \in [0, 20]$  after rescaling nucleotide indices). To state  $i \in \{1, 2\}$ , we assign a rate  $\lambda_i$ , which together with  $S(t)$ , defines a piecewise-constant rate function  $\lambda_{S(t)}$ . We model the Chi-site positions as drawn from a Poisson process with rate  $\lambda_{S(t)}$ , resulting in a Markov-modulated Poisson process [26]. MJP transitions from state 1 to state 2 have rate  $\alpha$  while transitions from state 2 to state 1 have rate  $\beta$ . We place gamma priors are placed for the four model

**Figure 9.** ESS/sec for  $(\alpha, \lambda_1)$  for the E. Coli data. The circles (in blue) are our proposed sampler as we vary the variance of the proposal distribution. The straight line is the Gibbs sampler.



parameters; specifically, we use  $\text{Gamma}(2, 2)$ ,  $\text{Gamma}(2, 3)$ ,  $\text{Gamma}(3, 2)$ ,  $\text{Gamma}(1, 2)$  for  $\alpha$ ,  $\beta$ ,  $\lambda_1$ ,  $\lambda_2$  respectively.

We use this setup to evaluate our symmetrized MH sampler along with Gibbs sampling (other algorithms perform much worse). For our MH proposal distribution, we first run 500 iterations of Gibbs sampling to estimate the posterior covariance of the vector  $\theta = (\alpha, \beta, \lambda_1, \lambda_2)$ , call this  $\Sigma_\theta$ . Our MH proposal distribution is then  $q(\nu|\theta) = N(\nu|\theta, \kappa\Sigma_\theta)$  for different settings of  $\kappa$  (the typical choice is  $\kappa = 1$ ). Figure 9 shows the results for parameters  $(\alpha, \lambda_1)$ , which are both very similar. We see that for the typical setting of  $\kappa = 1$ , our sampler outperforms the Gibbs sampler, though Gibbs sampling does outperform our method for large or small  $\kappa$ . This is because a) large or small  $\kappa$  mean the proposal variance is too large or too small, and b) the Gibbs conditionals over the parameters are conjugate for this model. Again, we expect the improvements our method offers to be more robust to the proposal distribution for more complex models without such conditional conjugacy.

## 7. Geometric ergodicity

Finally, we derive conditions under which our symmetrized MH algorithm inherits mixing properties of an ‘ideal’ sampler that operates without computational constraints. The latter proposes a new parameter  $\vartheta$  from distribution  $q(\vartheta|\theta)$ , and accepts with probability  $\alpha_I(\theta, \vartheta; X) = 1 \wedge \frac{P(X, \vartheta)q(\theta|\vartheta)}{P(X, \theta)q(\vartheta|\theta)}$ . The resulting ideal (but intractable) Markov chain has transition probability  $P_I(\theta'|\theta) = q(\theta'|\theta)\alpha_I(\theta, \theta'; X) + [1 - \int d\vartheta q(\vartheta|\theta)\alpha_I(\theta, \vartheta; X)]\delta_\theta(\theta')$ , the first term corresponding to acceptance, and the second, rejection.

Our main result is Theorem 3, which shows that if the ideal MCMC sampler is geometrically ergodic, then so is our tractable auxiliary variable sampler (Algorithm 5). We first state all our definitions and assumptions, before diving into the proofs.

**ASSUMPTION 1.** *The uniformization rate is set as  $\Omega(\theta, \vartheta) = \Omega(\theta) + \Omega(\vartheta)$ , where  $\Omega(\theta) = k_1 \max_s A_s(\theta) + k_0$ , for some  $k_1 > 1, k_0 > 0$ .*

Although it is possible to specify broader conditions under which our result holds, for clarity we focus on this case. We can drop the  $k_0$  if  $\inf_\theta \max_s A_s(\theta) > 0$

**ASSUMPTION 2.** *There exists a positive constant  $\theta_0$  such that for any  $\theta_x, \theta_y$  satisfying  $\|\theta_x\| \geq \|\theta_y\| > \theta_0$ , we have  $\Omega(\theta_x) \geq \Omega(\theta_y)$ .*

This assumption avoids book-keeping by making  $\Omega(\theta)$  increase monotonically with  $\theta$ .

DEFINITION 1. Let  $\pi_\theta$  be the stationary distribution of the MJP with rate-matrix  $A(\theta)$ , and define  $D_\theta = \text{diag}(\pi_\theta)$ . Define  $\tilde{A}(\theta) = D_\theta^{-1}A(\theta)D_\theta$ , and the reversibilization of  $A(\theta)$  as  $R_A(\theta) = (A(\theta) + \tilde{A}(\theta))/2$ .

This definition is from [8], who show that the matrix  $R_A(\theta)$  is reversible with real eigenvalues, the smallest being 0. The larger its second smallest eigenvalue, the faster the MJP converges to its stationary distribution  $\pi_\theta$ . Note that if the original MJP is reversible, then  $R_A(\theta) = A(\theta)$ .

ASSUMPTION 3. Write  $\lambda_2^{R_A}(\theta)$  for the second smallest eigenvalue of  $R_A(\theta)$ . There exist  $\mu > 0, \theta_1 > 0$  such that for all  $\theta$  satisfying  $\|\theta\| > \theta_1$ , we have  $\lambda_2^{R_A}(\theta) \geq \mu \max_s A_s(\theta)$  (or equivalently from Assumption 1,  $\lambda_2^{R_A}(\theta) \geq \mu \Omega(\theta)$ ), and  $\min_s \pi_\theta(s) > 0$ .

The assumption on  $\lambda_2^{R_A}$  is the strongest we need, requiring that  $\lambda_2^{R_A}(\theta)$  (which sets the MJP mixing rate) grows at least as fast as  $\max A_s(\theta)$ . This is satisfied when, for example, all elements of  $A(\theta)$  grow with  $\theta$  at similar rates, controlling the relative stability of the least and most stable states. While not trivial, this is a reasonable assumption: the MCMC chain over MJP paths will mix well if we can control the mixing of the MJP itself. To better understand this, recall  $B(\theta, \theta') = I + \frac{A(\theta)}{\Omega(\theta, \theta')}$  is the transition matrix of the embedded Markov chain, and note it has the same stationary distribution  $\pi_\theta$  as  $A(\theta)$ . Define the reversibilization  $R_B(\theta, \theta')$  from  $B(\theta, \theta')$  just as we did  $R_A(\theta)$  from  $A(\theta)$ .

LEMMA 2. Let  $\|\theta\| > \max(\theta_0, \theta_1)$  and  $\theta'$  satisfy  $\frac{1}{K_0} \leq \frac{\Omega(\theta')}{\Omega(\theta)} \leq K_0$  with  $K_0$  satisfying  $(1 + \frac{1}{K_0})k_1 \geq 2$ . For all such  $(\theta, \theta')$ , the Markov chain with transition matrix  $B(\theta, \theta')$  converges geometrically to stationarity at a rate uniformly bounded away from 0.

PROOF. A little algebra gives  $R_B(\theta, \theta') = I + R_A(\theta)/\Omega(\theta, \theta')$ . It follows that both  $R_A$  and  $R_B$  share the same eigenvectors, with eigenvalues satisfying  $\lambda_{R_B}(\theta, \theta') = 1 - \frac{\lambda_{R_A}(\theta)}{\Omega(\theta, \theta')}$ . In particular, the second largest eigenvalue  $\lambda_2^{R_B}(\theta, \theta')$  of  $R_B$  and second smallest eigenvalue  $\lambda_2^{R_A}(\theta, \theta')$  of  $R_A$  satisfy  $\lambda_2^{R_B}(\theta, \theta') = 1 - \frac{\lambda_2^{R_A}(\theta)}{\Omega(\theta, \theta')}$ . Then, from assumptions 1 and 3, and the lemma's assumptions,  $1 - \lambda_2^{R_B}(\theta, \theta') = \frac{\lambda_2^{R_A}(\theta)}{\Omega(\theta, \theta')} \geq \frac{\lambda_2^{R_A}(\theta)}{(K_0+1)\Omega(\theta)} \geq \frac{\mu}{K_0+1}$ . Also,

$$\Omega(\theta, \theta') = \Omega(\theta) + \Omega(\theta') \geq (1 + \frac{1}{K_0})\Omega(\theta) > (1 + \frac{1}{K_0})k_1 \max_s A_s(\theta) \geq 2 \max_s A_s(\theta).$$

So for any state  $s$ , the diagonal element  $B_s(\theta, \theta') = 1 - \frac{A_s(\theta)}{\Omega(\theta, \theta')} > \frac{1}{2}$ . From [8], this diagonal property and the bound on  $1 - \lambda_2^{R_B}(\theta, \theta')$  give the result.  $\square$

Our overall proof strategy is to show that for  $\|\theta\|$  and  $W$  large enough, the conditions of Lemma 2 hold with high probability. We show that Lemma 2 then allows the distribution over latent states for the continuous-time MJP and its discrete-time counterpart embedded in  $W$  to be brought arbitrarily close to  $\pi_\theta$  (and thus to each other), allowing our sampler to inherit mixing properties of the ideal sampler. For the remaining  $\theta$  and  $W$ , we will exploit their boundedness to establish a ‘small-set condition’ where the MCMC algorithm forgets its state with some probability. These two conditions will be sufficient for geometric ergodicity. The next assumption states these small-set conditions for the ideal sampler.



ASSUMPTION 4. For the ideal sampler with transition probability  $p_I(\theta'|\theta)$ :

i) for each  $M$ , for the set  $B_M = \{\theta : \Omega(\theta) \leq M\}$ , there exists a probability measure  $\phi$  and a constant  $\kappa_1 > 0$  s.t.  $\alpha_I(\theta, \theta'; X)q(\theta'|\theta) \geq \kappa_1\phi(\theta')$  for  $\theta \in B_M$ . Thus  $B_M$  is a 1-small set.

ii) for  $M$  large enough,  $\exists \rho < 1$  s. t.  $\int \Omega(\nu)p_I(\nu|\theta)d\nu \leq (1 - \rho)\Omega(\theta) + L_I, \forall \theta \notin B_M$ .

These two conditions are standard small-set and drift conditions necessary for the ideal sampler to satisfy geometric ergodicity. The first implies that for  $\theta$  in  $B_M$ , the ideal sampler forgets its current location with probability  $\kappa_1$ . The second condition ensures that for  $\theta$  outside this set, the ideal sampler drifts towards  $B_M$ . These two conditions together imply geometric mixing with rate equal or faster than  $\kappa_1$  [15]. Observe that we have used  $\Omega(\theta)$  as the so-called Lyapunov-Foster function to define the drift condition for the ideal sampler. This is the most natural choice, though our proof can be tailored to different choices. Similarly, we could easily allow  $B_M$  to be an  $n$ -small set for any  $n \geq 1$  (so the ideal sampler needs  $n$  steps before it can forget its current value in  $B_M$ ); we restrict ourselves to the 1-small case for clarity.

ASSUMPTION 5.  $\exists u > \ell > 0$  s.t.  $\prod P(X|s_o, \theta) \in [\ell, u]$  for any state  $s_o$  and  $\theta$ .

This assumption follows [16], and holds if  $\theta$  does not include parameters of the observation process (or if so, the likelihood is finite and nonzero for all settings of  $\theta$ ). We can relax this assumption, though this will introduce technicalities unrelated to our focus, which is on complications in parameter inference arising from the continuous-time dynamics, rather than the observation process.

ASSUMPTION 6. Given the proposal density  $q(\nu|\theta)$ ,  $\exists \eta_0 > 0, \theta_2 > 0$  such that for  $\theta$  satisfying  $\|\theta\| > \theta_2$ ,  $\int_{\Theta} \Omega(\nu)^2 q(\nu|\theta)d\nu \leq \eta_0 \Omega(\theta)^2$ .

This mild requirement can be satisfied by choosing a proposal distribution  $q$  that does not attempt to explore large  $\theta$ 's too aggressively.

COROLLARY 1. Given the proposal density  $q(\nu|\theta)$ ,  $\exists \eta_1 > 0, \theta_2 > 0$  such that for  $\theta$  satisfying  $\|\theta\| > \theta_2$ ,  $\int_{\Theta} \Omega(\nu)q(\nu|\theta)d\nu \leq \eta_1 \Omega(\theta)$ .

PROOF. From assumption 6, we have  $\int_{\Theta} \Omega(\nu)^2 q(\nu|\theta)d\nu \leq \eta_0 \Omega(\theta)^2$  for  $\theta$  satisfying  $\|\theta\| > \theta_2$ . For such  $\theta$ , by the Cauchy-Schwarz inequality, we have

$$\left[ \int_{\Theta} \Omega(\nu)q(\nu|\theta)d\nu \right]^2 \leq \int_{\Theta} \Omega(\nu)^2 q(\nu|\theta)d\nu \cdot \int_{\Theta} q(\nu|\theta)d\nu \leq \eta_0 \Omega(\theta)^2.$$

So for  $\theta$  satisfying  $\|\theta\| > \theta_2$ , we have  $\int_{\Theta} \Omega(\nu)q(\nu|\theta)d\nu \leq \sqrt{\eta_0} \Omega(\theta)$ .  $\square$

We need two further assumptions on the proposal distribution  $q(\theta'|\theta)$ .

ASSUMPTION 7. For any  $\epsilon > 0$ , there exist finite  $M_\epsilon, \theta_{3,\epsilon}$  such that for  $\theta$  satisfying  $\|\theta\| > \theta_{3,\epsilon}$ , the condition  $q(\{\theta' : \frac{p(\theta')q(\theta|\theta')}{p(\theta)q(\theta'|\theta)} \leq M_\epsilon\}|\theta) > 1 - \epsilon$  holds.

This holds, when e.g.  $p(\theta)$  is a gamma distribution, and  $q(\theta'|\theta)$  is Gaussian.



ASSUMPTION 8. For any  $\epsilon > 0$  and  $K > 1$ , there exists  $\theta_{4,\epsilon}^K$  such that for  $\theta$  satisfying  $\|\theta\| > \theta_{4,\epsilon}^K$ , the condition  $q(\{\theta' : \frac{\Omega(\theta')}{\Omega(\theta)} \in [\frac{1}{K}, K]\}|\theta) > 1 - \epsilon$  holds.

This holds when e.g.  $q(\theta'|\theta)$  is a centered on  $\theta$  and has finite variance.

THEOREM 3. Under the above assumptions, our auxiliary variable MCMC sampler is geometrically ergodic.

PROOF. This theorem follows from two lemmas we will prove. Lemma 5 shows there exist small sets  $\{(W, \theta, \vartheta) : \lambda_1|W| + \Omega(\theta) < M\}$  for  $\lambda_1, M > 0$ , within which our sampler forgets its current state with some positive probability. Lemma 8 shows that for appropriate  $(\lambda_1, M)$ , our sampler drifts towards this set whenever outside. Together, these two results imply geometric ergodicity [15, Theorems 15.0.1 and Lemma 15.2.8]. If  $\sup_\theta \Omega(\theta) < \infty$ , we just need the small set  $\{(W, \theta, \vartheta : |W| < M\}$  for some  $M$ .  $\square$

For easier comparison with the ideal sampler, we begin an MCMC iteration from step 5 in Algorithm 5. Thus, our sampler operates on  $(\theta, \vartheta, W)$ , with  $\theta$  the current parameter,  $\vartheta$  the auxiliary variable, and  $W$  the Poisson grid. An MCMC iteration updates this to  $(\theta', \vartheta', W')$  by (a) sampling states  $V$  (or  $(S, T)$ ) with a backward pass, (b) discarding  $\vartheta$ , (c) sampling  $\nu$  from  $q(\nu|\theta)$ , (d) sampling  $U'$  given  $(\theta, \nu)$  and setting  $W' = T \cup U'$ , (e) proposing to swap  $(\theta, \nu)$  and then (f) accepting or rejecting with a forward pass. On acceptance,  $\theta' = \nu$  and  $\vartheta' = \theta$ , and on rejection,  $\theta' = \theta$  and  $\vartheta' = \nu$ . We write  $(\theta'', \vartheta'', W'')$  for the MCMC state after two iterations. Recall that step (a) actually assigns states  $V$  to  $W$ .  $T$  are the elements of  $W$  where  $V$  changes value, and  $S$  are the corresponding elements of  $V$ . The remaining elements  $U$  are the elements of  $W$  corresponding to self-transitions. For reference, we repeat some of our notation in the appendix.

We first bound self-transition probabilities of the embedded Markov chain from 0:

PROPOSITION 4. The posterior probability that the embedded Markov chain makes a self-transition,  $P(V_i = V_{i+1}|W, X, \theta, \vartheta) \geq \delta_1 > 0$ , for any  $\theta, \vartheta, W$ .

The proof (in the appendix) exploits the bounded likelihood from assumption 5. A simple by-product of the proof is the following corollary:

COROLLARY 2.  $P(V_{i+1} = s|V_s = s, W, X, \theta, \vartheta) \geq \delta_1 > 0$ , for any  $\theta, \vartheta, W, s$ .

LEMMA 5. For all  $M, h > 0$ , the set  $B_{h,M} = \{(W, \theta, \vartheta) : |W| \leq h, \theta \in B_M\}$  is a 2-small set under our proposed sampler. Thus, for all  $(W, \theta, \vartheta)$  in  $B_{h,M}$ , the two-step transition probability satisfies  $P(W'', \theta'', \vartheta''|W, \theta, \vartheta) \geq \rho_1 \phi_1(W'', \theta'', \vartheta'')$  for a constant  $\rho_1$  and a probability measure  $\phi_1$  independent of the initial state.

PROOF. Recall the definition of  $B_M$ , and of an  $n$ -small set from Assumption 4. The 1-step transition probability of our MCMC algorithm consists of two terms, corresponding to the proposed parameter being accepted and rejected. Discarding the latter, we have

$$P(W', \theta', \vartheta'|W, \theta, \vartheta, X) \geq \delta_\theta(\vartheta')q(\theta'|\theta) \sum_{S,T} P(S, T|W, \theta, \vartheta, X)P(W'|S, T, \theta, \theta')\alpha(\theta, \theta', W'; X)$$

Here we use the fact that given  $(S, T)$ ,  $P(W'|S, T, \theta, \theta', X)$  is independent of  $X$ . We further bound the summation over  $(S, T)$  by considering only the terms with  $S$  a constant. When this constant is state  $s^*$ , we write this as  $(S = [s^*], T = \emptyset)$ . This corresponds to  $|W|$  self-transitions after the starting state  $S_0 = s^*$ , so that

$$\begin{aligned} P(S = [s^*], T = \emptyset | W, \theta, \vartheta, X) &= P(S_0 = s^* | X, W, \theta, \vartheta) \prod_{i=0}^{|W|-1} P(V_{i+1} = s^* | V_i = s^*, X, W, \theta, \vartheta) \\ &\geq P(S_0 = s^* | X, W, \theta, \vartheta) \delta_1^{|W|} \end{aligned}$$

Here  $\delta_1$  is the lower bound from Corollary 2. With  $S(t)$  fixed at  $s^*$ ,  $W'$  is a Poisson process with rate  $\Omega(\theta') + \Omega(\theta) - A_{s^*}(\theta)$ . From the Poisson superposition theorem,

$$\begin{aligned} P(W' | S = [s^*], T = \emptyset, \theta', \theta) &\geq P(W' \text{ from PoissProc}(\Omega(\theta'))) P(\emptyset \text{ from PoissProc}(\Omega(\theta) - A_{s^*}(\theta))) \\ &\geq P(W' \text{ from PoissProc}(\Omega(\theta'))) P(\emptyset \text{ from PoissProc}(\Omega(\theta))) \\ &\geq P(W' \text{ from PoissProc}(\Omega(\theta'))) \exp(-Mt_{end}) \quad (\text{since for } \theta \in B_M, \Omega(\theta) \leq M). \end{aligned}$$

Thus we have

$$\begin{aligned} \sum_{S, T} P(S, T, W' | W, \theta, \vartheta, X) &\geq \sum_{s^*} P(S = [s^*], T = \emptyset | W, \theta, \vartheta, X) P(W' | S = [s^*], T = \emptyset, \theta', \theta) \\ &\geq \delta_1^{|W|} \exp(-Mt_{end}) P(W' \text{ from PoissProc}(\Omega(\theta'))) \end{aligned} \quad (1)$$

Finally we relate the acceptance rate to that of the ideal sampler:

$$\begin{aligned} \alpha(\theta, \theta', W'; X) &= 1 \wedge \frac{P(X | W', \theta', \theta) / P(X | \theta')}{P(X | W', \theta, \theta') / P(X | \theta)} \cdot \frac{P(X | \theta') q(\theta | \theta') p(\theta')}{P(X | \theta) q(\theta' | \theta) p(\theta)} \\ &\geq 1 \wedge \frac{\ell^2}{u^2} \cdot \frac{P(X | \theta') q(\theta | \theta') p(\theta')}{P(X | \theta) q(\theta' | \theta) p(\theta)} \geq \alpha_I(\theta, \theta'; X) \frac{\ell^2}{u^2}. \end{aligned} \quad (2)$$

Since by assumption  $|W| \leq h$ , and  $q(\theta' | \theta) \alpha_I(\theta, \theta'; X) \geq \kappa_1 \phi(\theta')$  (from assumption 4),

$$\begin{aligned} P(W', \theta', \vartheta' | W, \theta, \vartheta) &\geq \frac{\ell^2}{u^2} \delta_1^h \exp(-Mt_{end}) \delta_\theta(\vartheta') \kappa_1 P(W' \text{ from PoissProc}(\Omega(\theta'))) \phi(\theta') \\ &\doteq \rho_1 \delta_\theta(\vartheta') P(W' \text{ from PoissProc}(\Omega(\theta'))) \phi(\theta') \end{aligned}$$

Write  $F_{\text{Poiss}(a)}$  for the CDF of a rate- $a$  Poisson. The two-step transition satisfies

$$\begin{aligned} P(W'', \theta'', \vartheta'' | W, \theta, \vartheta) &\geq \int_{B_{h, M}} P(W'', \theta'', \vartheta'' | W', \theta', \vartheta') P(W', \theta', \vartheta' | W, \theta, \vartheta) dW' d\theta' d\vartheta' \\ &\geq \int_{B_{h, M}} \rho_1 \delta_{\theta'}(\vartheta'') P(W'' \text{ from PoissProc}(\Omega(\theta''))) \phi(\theta'') \\ &\quad \rho_1 \delta_\theta(\vartheta') P(W' \text{ from PoissProc}(\Omega(\theta'))) \phi(\theta') dW' d\theta' d\vartheta' \\ &\geq \rho_1^2 \phi(\theta'') P(W'' \text{ from PoissProc}(\Omega(\theta''))) \int_{B_{h, M}} \delta_{\theta'}(\vartheta'') F_{\text{Poiss}(\Omega(\theta'))}(h) \phi(\theta') d\theta' \\ &\geq \rho_1^2 P(W'' \text{ from PoissProc}(\Omega(\theta''))) \phi(\theta'') \phi(\vartheta'') F_{\text{Poiss}(\Omega(\vartheta''))}(h) \delta_{B_{h, M}}(\vartheta'') \\ &\geq \rho_1^2 P(W'' \text{ from PoissProc}(\Omega(\theta''))) \phi(\theta'') \phi(\vartheta'') \delta_{B_{h, M}}(\vartheta'') \exp(-\Omega(\vartheta'')) \end{aligned} \quad (3)$$

The last line uses  $F_{\text{Pois}(a)}(h) \geq F_{\text{Pois}(a)}(0) = \exp(-a) \forall a$ , and gives our result, with  $\phi_1(W'', \theta'', \vartheta'') \propto P(W'' \text{ from PoissProc}(\Omega(\theta'')) \phi(\theta'') \phi(\vartheta'') \delta_{B_{h,M}}(\vartheta'') \exp(-\Omega(\vartheta''))$ .  $\square$

We have established the small set condition: for any point inside  $B_{h,M}$  our sampler forgets its state with nonzero probability. We next establish a drift condition, showing that outside this small set, the algorithm drifts back towards it (Lemma 8). We first establish a result needed when  $\max_s |A_s(\theta)|$  is unbounded as  $\theta$  increases. This states that the acceptance probabilities of our sampler and the ideal sampler can be brought arbitrarily close outside a small set, so long as  $\Omega(\theta)$  and  $\Omega(\theta')$  are sufficiently close.

LEMMA 6. Suppose  $\frac{1}{K_0} \leq \frac{\Omega(\theta)}{\Omega(\theta')} \leq K_0$ , for  $K_0$  satisfying  $(1 + \frac{1}{K_0})k_1 \geq 2$  ( $k_1$  is from Assumption 1). Write  $|W^\downarrow|$  for the minimum number of elements of grid  $W$  between any successive pairs of observations. For any  $\epsilon > 0$ , there exist  $w_\epsilon^{K_0}, \theta_{5,\epsilon}^{K_0} > 0$  such that  $|P(X|W, \theta, \theta') - P(X|\theta)| < \epsilon$  for any  $(W, \theta)$  with  $|W^\downarrow| > w_\epsilon^{K_0}$  and  $\|\theta\| > \theta_{5,\epsilon}^{K_0}$ .

PROOF. From lemma 2, for all  $\theta, \theta'$  satisfying the lemma's assumptions, the Markov chain with transition matrix  $B(\theta, \theta')$  converges geometrically to stationarity distribution  $\pi_\theta$  at a rate uniformly bounded away from 0. By setting  $|W^\downarrow|$  large enough, for all such  $(\theta, \theta')$  and for any initial state, the Markov chain would have mixed between each pair of observations, with distribution over states returning arbitrarily close to  $\pi_\theta$ .

Write  $W_X$  for the indices of the grid  $W$  containing observations, and  $V_X$  for the Markov chain state at these times (illustrated in Section A.1 in the appendix). Let  $P_B(V_X|W, \theta, \theta')$  be the probability distribution over  $V_X$  under the Markov chain with transition matrix  $B$  given  $W$  and  $P_{st}(V_X|\theta)$  be the probability of  $V_X$  sampled independently under the stationary distribution. Let  $P(X|W, \theta, \theta')$  be the marginal probability of the observations  $X$  under that Markov chain  $B(\theta, \theta')$  given  $W$ . Dropping  $W$  and  $\theta'$  from notation,  $P(X|\theta)$  is the probability of the observations under the rate- $A(\theta)$  MJP.

From the first paragraph, for  $|W^\downarrow| > w_0$  for large enough  $w_0$ ,  $P_B(V_X|W, \theta, \theta')$  and  $P_{st}(V_X|\theta)$  can be brought  $\epsilon'$  close. Then for any  $W$  with  $|W^\downarrow| > w_0$ , we have

$$\begin{aligned} |P(X|W, \theta, \theta') - P_{st}(X|\theta)| &= \left| \sum_{V_X} P(X|V_X, \theta) [P_B(V_X|W, \theta, \theta') - P_{st}(V_X|\theta)] \right| \\ &\leq \sum_{V_X} P(X|V_X, \theta) |P_B(V_X|W, \theta, \theta') - P_{st}(V_X|\theta)| \leq \epsilon'', \end{aligned}$$

using  $P(X|V_X, \theta) \leq u$  (Assumption 5), and  $\sum_{V_X} |P_B(V_X|W, \theta, \theta') - P_{st}(V_X|\theta)| < \epsilon$ . For large  $\theta$ , we prove a similar result in the continuous case by uniformization. For any  $\theta'$ ,

$$P(X|\theta) = \int dW P(X|W, \theta, \theta') P(W|\theta, \theta') \quad (P(W|\theta, \theta') \text{ is a rate-}\Omega(\theta) + \Omega(\theta') \text{ Poisson process}).$$

We split this integral into two parts, one over the set  $\{|W^\downarrow| > w_0\}$ , and the second over its complement. On the former, for  $w_0$  large enough,  $|P(X|W, \theta, \theta') - P_{st}(X|\theta)| \leq \epsilon''$ . For  $\theta$  large enough,  $\{|W^\downarrow| > w_0\}$  occurs with arbitrarily high probability for any  $\theta'$ . Since the likelihood is bounded, the integral over the second set can be made arbitrarily small (say,  $\epsilon''$  again). Finally, from the triangle inequality,

$$\begin{aligned} |P(X|\theta) - P(X|W, \theta, \theta')| &\leq |P(X|\theta) - P_{st}(X|\theta)| + |P_{st}(X|\theta) - P(X|W, \theta, \theta')| \\ &\leq (\epsilon'' + \epsilon'') + \epsilon'' \doteq \epsilon \end{aligned}$$

PROPOSITION 7. Let  $(W, \theta, \vartheta)$  be the current state of the sampler. Then, for any  $\epsilon$ , there exists  $\theta_\epsilon > 0$  as well as a set  $E_\epsilon \subseteq \{(W', \theta') : |\alpha_I(\theta, \theta'; X) - \alpha(\theta, \theta'; W', X)| \leq \epsilon\}$ , such that for  $\theta$  satisfying  $\|\theta\| > \theta_\epsilon$  and any  $\vartheta$ , we have  $P(E_\epsilon | W, \theta, \vartheta) > 1 - \epsilon$ .

The previous lemma bounded the difference in probability of observations under the discrete-time and continuous-time processes. This result uses this to bound the acceptance probabilities of the ideal sampler, and our proposed sampler (where acceptance probabilities are calculated conditioned on the grid  $W$ ). See the appendix for the proof.

LEMMA 8. (*drift condition*) There exist  $\delta_2 \in (0, 1)$ ,  $\lambda_1 > 0$  and  $L > 0$  such that  $\mathbb{E}[\lambda_1 |W'| + \Omega(\theta') | W, \theta, \vartheta, X] \leq (1 - \delta_2)(\lambda_1 |W| + \Omega(\theta)) + L$ .

PROOF. Since  $W' = T \cup U'$ , we consider  $\mathbb{E}[|T| | W, \theta, \vartheta, X]$  and  $\mathbb{E}[|U'| | W, \theta, \vartheta, X]$  separately. An upper bound of  $\mathbb{E}[|T| | W, \theta, \vartheta, X]$  can be derived directly from proposition 4:

$$\mathbb{E}[|T| | W, \theta, \vartheta, X] = \mathbb{E}\left[\sum_{i=0}^{|W|-1} \mathbb{I}_{\{V_{i+1} \neq V_i\}} | W, \theta, \vartheta, X\right] \leq \sum_{i=0}^{|W|-1} (1 - \delta_1) = |W|(1 - \delta_1).$$

By corollary 1, there exist  $\eta_1, \theta_2$  such that for  $\|\theta\| > \theta_2$ ,  $\int \Omega(\nu)q(\nu|\theta)d\nu \leq \eta_1\Omega(\theta)$ . Then,

$$\begin{aligned} \mathbb{E}[|U'| | W, \theta, \vartheta, X] &= \mathbb{E}_{S,T,\nu}[\mathbb{E}[|U'| | S, T, W, \theta, \vartheta, \nu, X]] = \mathbb{E}_{S,T,\nu}[\mathbb{E}[|U'| | S, T, W, \theta, \nu]] \\ &\leq \mathbb{E}_{S,T,\nu}[t_{\text{end}}\Omega(\theta, \nu)] = t_{\text{end}} \int \Omega(\theta, \nu)q(\nu|\theta)d\nu \\ &= t_{\text{end}} \left[ \left( \Omega(\theta) + \int_{\Theta} \Omega(\nu)q(\nu|\theta)d\nu \right) \right] \leq t_{\text{end}}(\eta_1 + 1)\Omega(\theta) \end{aligned}$$

To bound  $\mathbb{E}[\Omega(\theta') | W, \theta, \vartheta, X]$ , consider the transition probability over  $(W', \theta')$ :

$$\begin{aligned} P(dW', d\theta' | W, \theta, \vartheta) &= d\theta' dW' \left[ q(\theta'|\theta) \sum_{S,T} P(S, T | W, \theta, \vartheta, X) P(W' | S, T, \theta, \theta') \alpha(\theta, \theta'; W', X) \right. \\ &\quad \left. + \int q(\nu|\theta) \sum_{S,T} P(S, T | W, \theta, \vartheta, X) P(W' | S, T, \theta, \nu) (1 - \alpha(\theta, \nu; W', X)) d\nu \delta_\theta(\theta') \right]. \end{aligned}$$

With  $P(W' | W, \theta, \vartheta, \theta', X) = \sum_{S,T} P(S, T | W, \theta, \vartheta, X) P(W' | S, T, \theta, \theta')$ , integrate out  $W'$ :

$$\begin{aligned} P(d\theta' | W, \theta, \vartheta) &= d\theta' \int_{W'} dW' \left[ q(\theta'|\theta) P(W' | W, \theta, \vartheta, \theta', X) \alpha(\theta, \theta'; W', X) + \right. \\ &\quad \left. \int q(\nu|\theta) P(W' | W, \theta, \vartheta, \nu, X) (1 - \alpha(\theta, \nu; W', X)) d\nu \delta_\theta(\theta') \right] \end{aligned}$$

Then let  $\int \Omega(\theta') P(d\theta' | W, \theta, \vartheta) = I_1(W, \theta, \vartheta) + \Omega(\theta) I_2(W, \theta, \vartheta)$ , with

$$\begin{aligned} I_1(W, \theta, \vartheta) &= \int d\theta' \Omega(\theta') q(\theta'|\theta) \int dW' P(W' | W, \theta, \vartheta, \theta', X) \alpha(\theta, \theta'; W', X), \\ I_2(W, \theta, \vartheta) &= \int d\nu dW' q(\nu|\theta) P(W' | W, \theta, \vartheta, \nu, X) (1 - \alpha(\theta, \nu; W', X)). \end{aligned}$$

Consider the second term  $I_2$ . From Proposition 7, for any positive  $\epsilon$ , there exists  $\theta_\epsilon > 0$  such that the set  $E_\epsilon$  (where  $|\alpha(\theta, \nu; X, W') - \alpha_I(\theta, \nu; X)| \leq \epsilon$ ) has probability greater than  $1 - \epsilon$ . Write  $I_{2,E_\epsilon}$  for the integral restricted to this set, and  $I_{2,E_\epsilon^c}$  for that over the complement, so that  $I_2 = I_{2,E_\epsilon} + I_{2,E_\epsilon^c}$ . Then for  $\theta > \theta_\epsilon$ ,

$$\begin{aligned} I_{2,E_\epsilon}(W, \theta, \vartheta) &= \int_{E_\epsilon} d\nu dW' q(\nu|\theta) P(W'|W, \theta, \vartheta, \nu, X) (1 - \alpha(\theta, \nu; W', X)) \\ &\leq \int_{E_\epsilon} d\nu dW' q(\nu|\theta) P(W'|W, \theta, \vartheta, \nu, X) [1 - (\alpha_I(\theta, \nu; X) - \epsilon)] \\ &\leq \int d\nu dW' q(\nu|\theta) P(W'|W, \theta, \vartheta, \nu, X) [1 - (\alpha_I(\theta, \nu; X) - \epsilon)] \\ &\leq (1 + \epsilon) - \int q(\nu|\theta) \alpha_I(\theta, \nu; X) d\nu, \quad \text{and} \\ I_{2,E_\epsilon^c}(W, \theta, \vartheta) &= \int_{E_\epsilon^c} d\nu dW' q(\nu|\theta) P(W'|W, \theta, \vartheta, \nu, X) (1 - \alpha(\theta, \nu; W', X)) \\ &\leq \int_{E_\epsilon^c} d\nu dW' q(\nu|\theta) P(W'|W, \theta, \vartheta, \nu, X) \leq \epsilon. \end{aligned}$$

We similarly divide the integral  $I_1$  into two parts,  $I_{1,E_\epsilon}$  (over  $E_\epsilon$ ) and  $I_{1,E_\epsilon^c}$  (over its complement  $E_\epsilon^c$ ). For  $\|\theta\|$  large enough, we can bound the acceptance probability by  $\alpha_I(\theta, \theta'; X) + \epsilon$  on the set  $E_\epsilon$ , and by corollary 1, we get

$$I_{1,E_\epsilon} \leq \int_{E_\epsilon} \Omega(\theta') q(\theta'|\theta) (\alpha_I(\theta, \theta'; X) + \epsilon) d\theta' \leq \int \Omega(\theta') q(\theta'|\theta) \alpha_I(\theta, \theta'; X) d\theta' + \eta_1 \epsilon \Omega(\theta).$$

For  $I_{1,E_\epsilon^c}$ , from assumption 6, we have  $\int_{\Theta} \Omega(\nu)^2 q(\nu|\theta) d\nu \leq \eta_0 \Omega(\theta)^2$  for  $\|\theta\| > \theta_2$ . So, by Cauchy-Schwarz inequality and bounding the acceptance probability by one, we have

$$\begin{aligned} (I_{1,E_\epsilon^c})^2 &\leq \int_{E_\epsilon^c} q(\theta'|\theta) P(W'|W, \theta, \vartheta, \theta', X) d\theta' dW' \int_{E_\epsilon^c} \Omega(\theta')^2 q(\theta'|\theta) P(W'|W, \theta, \vartheta, \theta', X) d\theta' dW' \\ &\leq \epsilon \int \Omega(\theta')^2 q(\theta'|\theta) d\theta' \leq \epsilon \eta_0 \Omega(\theta)^2, \end{aligned}$$

giving  $I_{1,E_\epsilon^c} \leq \sqrt{\epsilon \eta_0} \Omega(\theta)$ . Putting these four results together, for  $\theta$  satisfying  $\|\theta\| > \max(\theta_2, \theta_\epsilon, M)$  (where  $M$  is from Assumption 4 on the ideal sampler), we have

$$\begin{aligned} \int \Omega(\theta') P(d\theta'|W, \theta, \vartheta) &\leq \int \Omega(\theta') q(\theta'|\theta) \alpha_I(\theta, \theta'|X) d\theta' + \Omega(\theta) \int q(\nu|\theta) (1 - \alpha_I(\theta, \nu|X)) d\nu + \\ &\quad \sqrt{\eta_0 \epsilon} \Omega(\theta) + \eta_1 \epsilon \Omega(\theta) + 2\epsilon \Omega(\theta) \\ &\leq (1 - \rho) \Omega(\theta) + (\sqrt{\eta_0 \epsilon} + \eta_1 \epsilon + 2\epsilon) \Omega(\theta) + L_I, \quad \text{giving} \end{aligned}$$

$$\begin{aligned} \mathbb{E}[\lambda_1 | W'] + \Omega(\theta') | W, \theta, \vartheta, X] &\leq \lambda_1 (1 - \delta_1) |W| + \lambda_1 t_{end} (1 + \eta_1) \Omega(\theta) \\ &\quad + (1 - \rho) \Omega(\theta) + (\sqrt{\eta_0 \epsilon} + \eta_1 \epsilon + 2\epsilon) \Omega(\theta) + L_I \\ &= (1 - \delta_1) \lambda_1 |W| + [1 - (\rho - \lambda_1 t_{end} (1 + \eta_1) - (2 + \eta_1) \epsilon - \sqrt{\eta_0 \epsilon})] \Omega(\theta) + L_I \\ &\doteq (1 - \delta_1) \lambda_1 |W| + (1 - \delta_2) \Omega(\theta) + L_I \end{aligned}$$

For  $(\lambda_1, \epsilon)$  small enough,  $\delta_2 \in (0, 1)$ , and  $\delta = \min(\delta_1, \delta_2)$  gives the drift condition.  $\square$

## 8. Conclusion

We have proposed a novel Metropolis-Hastings algorithm for parameter inference in Markov jump processes. We use uniformization to update the MJP parameters with state-values marginalized out, though still conditioning on a random Poisson grid. The distribution of this grid depends on the MJP parameters, significantly slowing down MCMC mixing. We propose a novel symmetrization scheme to get around this dependency. In our experiments, we demonstrate the usefulness of this scheme, which outperforms a number of competing baselines. We also derive conditions under which our sampler inherits geometric ergodicity properties of an ideal MCMC sampler.

There are a number of interesting directions for future research. Our focus was on Metropolis-Hastings algorithms for typical settings, where the parameters are low dimensional. It is interesting to investigate how our ideas extend to schemes like Hamiltonian Monte Carlo [19] suited for higher-dimensional settings. Another direction is to develop and study similar schemes for more complicated hierarchical models like mixtures of MJPs or coupled MJPs. While we focused only on Markov jump processes, it is also of interest to study similar ideas for algorithms for more general processes [24]. It is also important to investigate how similar ideas apply to deterministic algorithms like variational Bayes [20, 22]. From a theoretical viewpoint, our proof required the uniformization rate to satisfy  $\Omega(\theta) \geq k_1 \max_s A_s(\theta) + k_0$  for  $k_1 > 1$ . We believe our result still holds for  $k_1 = 1$ , and for completeness, it would be interesting to prove this.

## References

- [1] C. Andrieu, A. Doucet, and R. Holenstein. Particle Markov chain Monte Carlo methods. *Journal of the Royal Statistical Society*, B, 2010.
- [2] C. Andrieu and G. O. Roberts. The pseudo-marginal approach for efficient Monte Carlo computations. *Annals of Statistics*, 37(2), 2009.
- [3] L. Breuer. *From Markov jump processes to spatial queues*. Springer, 2003.
- [4] E. Çinlar. *Introduction to Stochastic Processes*. Prentice Hall, 1975.
- [5] T. El-Hay, N. Friedman, and R. Kupferman. Gibbs sampling in factorized continuous-time Markov processes. In *UAI*, pages 169–178, 2008.
- [6] R. Elliott and C. J. Osakwe. Option pricing for pure jump processes with Markov switching compensators. *Finance and Stochastics*, 10:250–275, 2006.
- [7] P. Fearnhead and C. Sherlock. An exact Gibbs sampler for the Markov-modulated Poisson process. *Journal Of the Royal Statistical Society Series B*, 68(5):767–784, 2006.
- [8] J. A. Fill. Eigenvalue bounds on convergence to stationarity for nonreversible Markov chains, with an application to the exclusion process. *Ann. Appl. Probab.*, 1(1):62–87, 02 1991.

- [9] D. T. Gillespie. Exact stochastic simulation of coupled chemical reactions. *The Journal of Physical Chemistry*, 81(25):2340–2361, 1977.
- [10] N. Goldman and Z. Yang. A codon-based model of nucleotide substitution for protein-coding DNA sequences. *Molecular biology and evolution*, 11(5):725–736, 1994.
- [11] D. Gross, J.F. Shortle, J.M. Thompson, and C.M. Harris. *Fundamentals of Queueing Theory*. Wiley Series in Probability and Statistics. Wiley, 2011.
- [12] A. Hobolth and E. Stone. Simulation from endpoint-conditioned, continuous-time Markov chains on a finite state space, with applications to molecular evolution. *Ann Appl Stat*, 3(3):1204, 2009.
- [13] A. Jensen. Markoff chains as an aid in the study of Markoff processes. *Skand. Aktuarietiedskr.*, 36:87–91, 1953.
- [14] T. H. Jukes and C. R. Cantor. *Evolution of Protein Molecules*. Academy Press, 1969.
- [15] S. Meyn and R. L. Tweedie. *Markov Chains and Stochastic Stability*. Cambridge University Press, New York, NY, USA, 2nd edition, 2009.
- [16] B. Miasojedow and W. Niemiro. Geometric ergodicity of Rao and Tehs algorithm for Markov jump processes and CTBNs. *Electron. J. Statist.*, 11(2):4629–4648, 2017.
- [17] J. Møller, A. N. Pettitt, R. Reeves, and K. K. Berthelsen. An efficient Markov chain Monte Carlo method for distributions with intractable normalising constants. *Biometrika*, 93(2):451–458, 2006.
- [18] I. Murray, Z. Ghahramani, and D. J. C. MacKay. MCMC for doubly-intractable distributions. In *Proceedings of the 22nd Annual Conference on Uncertainty in Artificial Intelligence (UAI-06)*, pages 359–366. AUAI Press, 2006.
- [19] R. M. Neal. MCMC using Hamiltonian dynamics. *Handbook of Markov Chain Monte Carlo*, 54:113–162, 2010.
- [20] M. Opper and G. Sanguinetti. Variational inference for Markov jump processes. In *Neural Information Processing Systems*, 2007.
- [21] J. Pan, V. Rao, P. K. Agarwal, and A. E. Gelfand. Markov-modulated marked Poisson processes for check-in data. In *Proc. of the 33rd Intern. Conf. on Mach. Learning*, 2016.
- [22] J. Pan, B. Zhang, and V. Rao. Collapsed variational bayes for Markov jump processes. In *Neural Information Processing systems*, 2017.
- [23] M. Plummer, N. Best, K. Cowles, and K. Vines. CODA: Convergence diagnosis and output analysis for MCMC. *R News*, 6(1):7–11, March 2006.
- [24] V. Rao and Y. W. Teh. MCMC for continuous-time discrete-state systems. In *Advances in Neural Information Processing Systems*, (24), 2012.

- [25] V. Rao and Y. W. Teh. Fast MCMC sampling for Markov jump processes and extensions. *Journal of Machine Learning Research*, 2013.
- [26] S. L. Scott and P. Smyth. The Markov modulated Poisson process and Markov Poisson cascade with applications to web traffic modeling. *Bayesian Statistics*, 7:1–10, 2003.
- [27] J. Xu and C. R. Shelton. Intrusion detection using continuous time Bayesian networks. *Journal of Artificial Intelligence Research*, 39:745–774, 2010.

## A. Appendix

### A.1. Notation

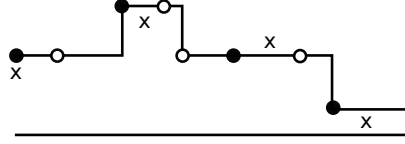


**Figure 10.** an example MJP path

We recall some notation used in our proof. The figure about shows a realization  $S(t)$  of an MJP with rate matrix  $A(\theta)$  and initial distribution  $\pi_0$  over an interval  $[0, t_{end}]$ . The crosses are observations  $X$ .  $\pi_0$  is the initial distribution over states, and  $\pi_\theta$  is the stationary distribution of the MJP.  $p(\theta)$  is the prior over  $\theta$ , and  $q(\nu|\theta)$  is the proposal distribution.

- The uniformized representation of  $S(t)$  is the pair  $(V, W)$ , with the Poisson grid  $W = [w_1, w_2, w_3, w_4, w_5, w_6, w_7]$  and the states  $V = [v_0, v_1, v_2, v_3, v_4, v_5, v_6, v_7]$  assigned with through a Markov chain with initial distribution  $\pi_0$  and transition matrix  $B(\theta, \theta')$ . In the figure, the circles (filled and empty) correspond to  $W$ .
- The more standard representation of  $S(t)$  is the pair  $(S, T)$ . Here  $T$  are the elements of  $W$  which are true jump times (when  $V$  changes value), and  $S$  are the corresponding elements of  $V$ .  $U$  are the remaining elements of  $W$  corresponding to self-transitions. Here,  $T = [w_2, w_4, w_7]$  and  $U = [w_1, w_3, w_5, w_6]$ .
- The filled circles represent  $W_X$ , which are the elements of  $W$  containing observations.  $V_X$  are the states corresponding to  $W_X$ . In this example,  $W_X = [w_2, w_5, w_7] \cup \{0\}$  and  $V_X = [v_2, v_5, v_7] \cup \{v_0\}$ .
- We write  $|W^\downarrow|$  for the minimum number of elements of  $W$  between successive pairs of observations (including start time 0). In this example,  $|W^\downarrow| = \min(3, 3, 2) = 2$ .



- $P(X|W, \theta, \theta')$  is the marginal distribution of  $X$  on  $W$  under a Markov chain with transition matrix  $B(\theta, \theta')$  (after integrating out the state information  $V$ ). Recall that the LHS does not depend on  $\theta'$  because of uniformization.
- $P(X|\theta)$  is the marginal probability of the observations under the rate- $A(\theta)$  MJP.  $P(X|\theta) = \int_W P(X|W, \theta, \theta')P(W|\theta, \theta')dW$ .
- $P_B(V_X|W, \theta, \theta')$  is the probability distribution over states  $V_X$  for the Markov chain with transition matrix  $B(\theta, \theta')$  on the grid  $W$ , with the remaining elements of  $V$  integrated out.
- $P_{st}(V_X|\theta)$  is the probability of  $V_X$  when elements of  $V_X$  are sampled i.i.d. from  $\pi_\theta$ .
- $P_{st}(X|\theta)$  is the marginal probability of  $X$  when  $V_X$  is drawn from  $P_{st}(V_X|\theta)$ .

### A.2. Remaining proofs

PROPOSITION 4. *The a posteriori probability that the embedded Markov chain makes a self-transition,  $P(V_{i+1} = V_i|W, X, \theta, \vartheta) \geq \delta_1 > 0$ , for any  $\theta, \vartheta, W$ .*

PROOF. We use  $k_0$  from assumption 1 to bound *a priori* self-transition probabilities:

$$P(V_{i+1} = s|V_i = s, W, \theta, \vartheta) = B_{ss}(\theta, \vartheta) = 1 - \frac{A_s(\theta)}{\Omega(\theta, \vartheta)} \geq 1 - \frac{A_s(\theta)}{\Omega(\theta)} \geq 1 - \frac{1}{k_0}.$$

We then have

$$\begin{aligned} P(V_i = V_{i+1}|W, X, \theta, \vartheta) &= \sum_v P(V_i = V_{i+1} = v|W, X, \theta, \vartheta) = \sum_v \frac{P(V_i = V_{i+1} = v, X|W, \theta, \vartheta)}{P(X|W, \theta, \vartheta)} \\ &= \sum_v \frac{P(X|V_i = V_{i+1} = v, W, \theta, \vartheta)P(V_i = V_{i+1} = v|W, \theta, \vartheta)}{P(X|W, \theta, \vartheta)} \\ &\geq \frac{\ell}{u} \sum_v P(V_i = V_{i+1} = v|W, \theta, \vartheta) \\ &= \frac{\ell}{u} \sum_v P(V_{i+1} = v|V_i = v, W, \theta, \vartheta)P(V_i = v|\theta, \vartheta) \\ &\geq \frac{\ell}{u} \left(1 - \frac{1}{k_0}\right) \doteq \delta_1 > 0. \end{aligned}$$

□

PROPOSITION 7. *Let  $(W, \theta, \vartheta)$  be the current state of the sampler. Then, for any  $\epsilon$ , there exists  $\theta_\epsilon > 0$  as well as a set  $E_\epsilon \subseteq \{(W', \theta') : |\alpha_I(\theta, \theta'; X) - \alpha(\theta, \theta'; W', X)| \leq \epsilon\}$ , such that for  $\theta$  satisfying  $\|\theta\| > \theta_\epsilon$  and any  $\vartheta$ , we have  $P(E_\epsilon|W, \theta, \vartheta) > 1 - \epsilon$ .*

PROOF. Fix  $\epsilon > 0$  and  $K > 1$  satisfying  $(1 + \frac{1}{K})k_1 \geq 2$ .

- From assumption 7, there exist  $M_\epsilon$  and  $\theta_{1,\epsilon}$ , such that  $P(\frac{q(\theta|\theta')p(\theta')}{q(\theta'|\theta)p(\theta)} \leq M_\epsilon) > 1 - \epsilon/2$  for  $\theta$  satisfying  $\|\theta\| > \theta_{1,\epsilon}$ . Define  $E_1^\epsilon = \{\theta' \text{ s.t. } \frac{q(\theta|\theta')p(\theta')}{q(\theta'|\theta)p(\theta)} \leq M_\epsilon\}$ .

- Define  $E_2^K = \{\theta' \text{ s.t. } \frac{\Omega(\theta')}{\Omega(\theta)} \in [1/K, K]\}$ . Following assumption 8, define  $\theta_{2,\epsilon}^K$  such that  $P(E_2^K|\theta) > 1 - \epsilon/2$  for all  $\theta$  satisfying  $\|\theta\| > \theta_{2,\epsilon}^K$ .
- On the set  $E_2^K$ ,  $\Omega(\theta') \leq K\Omega(\theta)$  (and also  $\Omega(\theta) \leq K\Omega(\theta')$ ). Lemma 6 ensures that there exist  $\theta_{3,\epsilon}^K > 0, w_\epsilon^K > 0$ , such that for  $|W^\downarrow| > w_\epsilon^K$ ,  $\|\theta\| > \theta_{3,\epsilon}^K$  and  $\|\theta'\| > \theta_{3,\epsilon}^K$ , we have  $|P(X|W, \theta', \theta) - P(X|\theta')| < \epsilon$ , and  $|P(X|W, \theta, \theta') - P(X|\theta)| < \epsilon$ . Define  $E_{3,\epsilon}^K = \{\theta' \text{ s.t. } \|\theta'\| > \theta_{3,\epsilon}^K\}$ .
- Define  $E_{4,\epsilon}^K = \{W \text{ s.t. } |W^\downarrow| > w_\epsilon^K\}$ . Set  $\theta_{4,\epsilon}^K$ , so that for  $\|\theta\| > \theta_{4,\epsilon}^K$ ,  $P(E_{4,\epsilon}^K|E_2^K, E_1^\epsilon) > 1 - \epsilon$ . This holds since  $W$  comes from a Poisson processes, whose rate can be made arbitrarily large by increasing  $\Omega(\theta)$ .
- From assumption 2, there exists  $\theta_0$ , such that  $\Omega(\theta)$  increases as  $\|\theta\|$  increases, for  $\theta$  satisfying  $\|\theta\| > \theta_0$ . Set  $\theta_\epsilon = \max(\theta_0, \theta_{1,\epsilon}, \theta_{2,\epsilon}^K, \theta_{3,\epsilon}^K, \theta_{4,\epsilon}^K)$ .

Now consider the difference

$$\begin{aligned} |\alpha(\theta, \theta'; W, X) - \alpha_I(\theta, \theta'; X)| &= \left| 1 \wedge \frac{P(X|W, \theta', \theta)q(\theta|\theta')p(\theta')}{P(X|W, \theta, \theta')q(\theta'|\theta)p(\theta)} - 1 \wedge \frac{P(X|\theta')q(\theta|\theta')p(\theta')}{P(X|\theta)q(\theta'|\theta)p(\theta)} \right| \\ &\leq \left| \frac{P(X|W, \theta', \theta)}{P(X|W, \theta, \theta')} - \frac{P(X|\theta')}{P(X|\theta)} \right| \frac{q(\theta|\theta')p(\theta')}{q(\theta'|\theta)p(\theta)}. \end{aligned}$$

On  $E_1^\epsilon$ ,  $\frac{q(\theta|\theta')p(\theta')}{q(\theta'|\theta)p(\theta)} \leq M_\epsilon$ . Since  $P(X|W, \theta, \theta')$  and  $P(X|\theta)$  are lower-bounded by  $\ell$ , for any  $\epsilon > 0$  we can find a  $K$  such that on  $E_2^K \cap E_{3,\epsilon}^K$ ,

$$\left| \frac{P(X|W, \theta', \theta)}{P(X|W, \theta, \theta')} - \frac{P(X|\theta')}{P(X|\theta)} \right| < \epsilon/M_\epsilon.$$

This means that on  $E_1^\epsilon \cap E_2^K \cap E_{3,\epsilon}^K$ ,  $|\alpha(\theta, \theta', W, X) - \alpha_I(\theta, \theta', X)| < \epsilon$ .

For  $\theta > \max(\theta_{1,\epsilon}, \theta_{2,\epsilon}^K)$  we have  $P(E_2^K E_1^\epsilon) \geq P(E_2^K) + P(E_1^\epsilon) - 1 \geq 1 - \epsilon$ .

When  $E_2^K$  holds,  $\Omega(\theta') \geq \Omega(\theta)/K$ . For  $\theta$  large enough, we can ensure  $\|\theta'\| > \theta_{3,\epsilon}^K$ . So

$$P(E_1^\epsilon E_2^K E_{3,\epsilon}^K E_{4,\epsilon}^K) > (1 - \epsilon)^2.$$

Finally, set  $E_\epsilon \doteq E_1^\epsilon \cap E_2^K \cap E_{3,\epsilon}^K \cap E_{4,\epsilon}^K$ , giving us our result.

## A.3. Algorithm sketch

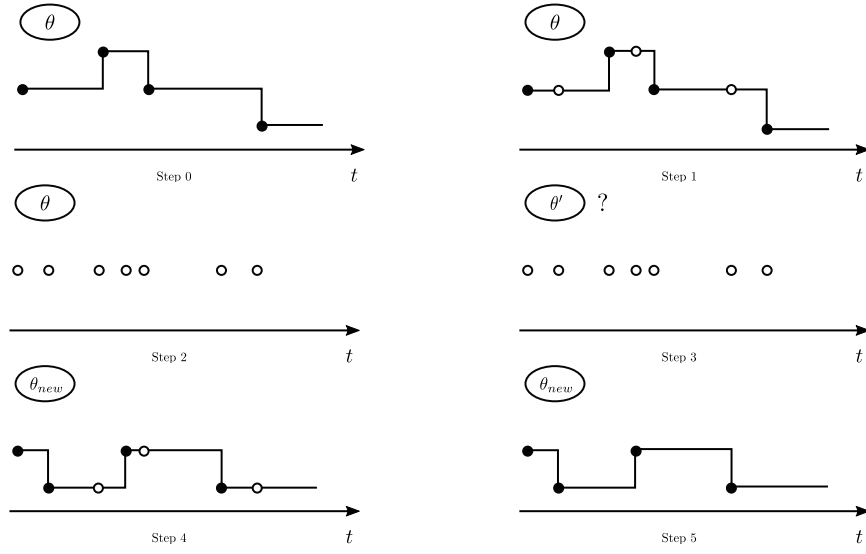


**Figure 11.** Naïve MH-algorithm: Step 0 to 2: sample thinned events and discard state information to get a random grid. Step 3: propose a new parameter  $\theta'$ , and accept or reject by making a forward pass on the grid. Steps 4 to 5: make a backward pass using the accepted parameter and discard self-transitions to produce a new trajectory.

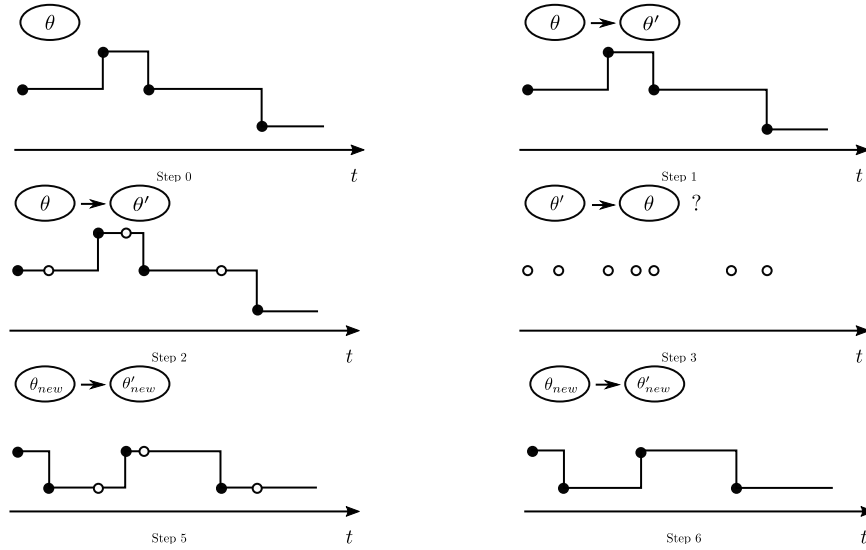


**Figure 12.** Improved MH algorithm: Steps 0-3: Starting with a trajectory and parameter  $\theta$ , simulate an auxiliary parameter  $\theta^*$ , and then the thinned events  $U$  from a rate  $\Omega(\theta) + \Omega(\theta^*) - A_{S(t)}$  Poisson process. Step 4: Propose swapping  $\theta$  and  $\theta^*$ . Step 5: Run a forward pass to accept or reject this proposal, and use the accepted parameter to simulate a new trajectory. Step 6: Discard the thinned events.

## A.4. Additional results

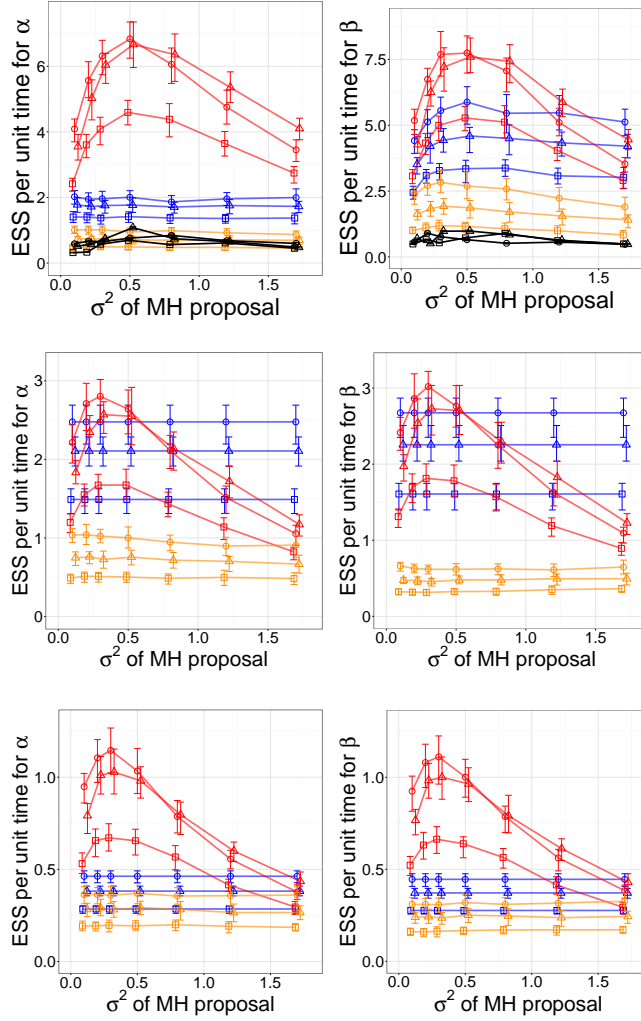


**Figure 13.** ESS/sec for the synthetic model, dimension 5. The left column is for  $\alpha$ , and the right is for  $\beta$ . Red, yellow, blue and black curves are the symmetrized MH, naïve MH, Gibbs and particle MCMC algorithm. Different symbols correspond to different settings of the algorithms, see section 6.

**Figure 14.** ESS/sec for the immigration model, the top row being dimension 5. The left column is for  $\alpha$ , and the right is for  $\beta$ . Red, yellow, and blue curves are the symmetrized MH, naïve MH, Gibbs sampling and particle MCMC.

**Figure 15.** ESS/sec for the time-inhomogeneous immigration model, the top row being dimension 5. The left column is for  $\alpha$ , and the right is for  $\beta$ . Red, yellow and blue curves are the symmetrized MH, naïve MH, and Gibbs algorithm.